1975

Physical studies of unfolded 30S ribosomal subunits of Escherichia coli

Donald Preston Blair
The University of Montana

PHYSICAL STUDIES OF UNFOLDED 30S RIBOSOMAL SUBUNITS OF *ESCHERICHIA COLI*

by

Donald P. Blair

B. A., University of Montana, 1970

Presented in partial fulfillment of the requirements for the degree of

Masters of Science

UNIVERSITY OF MONTANA

1975

Approved by:

Walter E. Hill
Chairman, Board of Examiners

K C Murray
Dean, Graduate School

3-2-78
Date

ProQuest LLC.
789 East Eisenhower Parkway
P.O. Box 1346
Ann Arbor, MI 48106 - 1346

3

Blair, Donald P., M.S., June 1978 Chemistry

Physical Studies of Unfolded 30S Ribosomal Subunits of Escherichia Coli (91 pp.)

Director: Walter E. Hill

The 30S ribosomal subunit of Escherichia coli undergoes an extensive conformational change upon exposure to low Mg^{++} concentration. Dialysis of the subunit against a buffer containing 0.0001 M $MgCl_2$, 0.07 M KCl, 0.01 M Tris-HCl, pH 7.4, resulted in an unfolded particle that was characterized by determining a number of its physical parameters. As determined in this study, the $s^{\circ}_{20,w}$ of the unfolded subunit was 23.3 ± 0.3, the partial specific volume was 0.619 ± 0.006 ml/g, the intrinsic viscosity was 11.0 ± 0.2 ml/g, and the extinction coefficient at 260 nm was 145. The unfolded particles consisted of 33 ± 2% protein and 65 ± 2% RNA. Acrylamide gel electrophoresis indicated no loss of protein in the unfolded subunit.

The 30S subunit exhibits a decrease in sedimentation coefficient and an increase in intrinsic viscosity when exposed to low Mg^{++} concentration. The large change that occurs in these physical parameters indicates that the unfolded subunit is more asymmetric and/or hydrated than the 30S subunit. Based on the assumption that the hydration is unchanged from the 30S subunit, the 23S particle has a calculated axial ratio of approximately 7:1. The asymmetry of this particle can best be explained by assuming that a portion of the RNA chain swings out resulting in an extended conformation.

Solutions of the 23S particle were also subjected to sonication for 20-25 minutes in an attempt to break off the unfolded portion of the subunit. The sonication produced 3 particles that were isolated and analyzed for protein and RNA content. The three particles had approximate sedimentation coefficients of 5S, 10S, and 15S and were found to have protein/RNA ratios of 0.16, 0.49, and 0.49, respectively. From gel electrophoresis, it was found that the 10S particles had 13 proteins, and the 15S particles had 15 proteins. No protein bands were observed from the 5S particle. Unique proteins were found on the 10S and 15S particles. Four proteins in the 10S particle were not contained in the 15S particle, and six proteins in the 15S particle were not contained in the 10S particle. The sonication appears to break the unfolded subunit into at least two different particles, each of which contain a unique protein content.

ACKNOWLEDGMENTS

The author would like to thank Dr. Walter E. Hill for his support and guidance throughout the course of this study. I would also like to thank Curtis Nessit and Larry Heilmann for their help in preparation of the ribosomes.

TABLE OF CONTENTS

LIST OF TABLES

LIST OF FIGURES

CHAPTER I

INTRODUCTION

In 1943, Luria, Delbruk, and Anderson (75) reported observing an abundance of small, uniform particles in the electron micrographs of cytoplasm from lysed bacteria. These particles were found in extracts of all bacterial cells examined (5, 113) and were found to contain most of the ribonucleic acid (RNA) of the cells as well as some proteins (113). The chemical composition and size of these ribonucleoprotein (RNP) particles resembled the particles studied extensively in animal tissues (101, 102, 103, 105, 106), in plants (143, 144), and in yeast (17, 18). These ribonucleoprotein particles are now called ribosomes.

These particles were observed to be somewhat spherical with a diameter of about 100 to 200 angstroms (Å) and were composed of RNA and protein approximately in the ratio of 2 to 1. They were generally thought to be involved in protein synthesis (72, 73). One of the most prominent features of these particles was that under certain conditions they would dissociate into unequal subunits. This phenomenon led to the finding that the divalent cation, magnesium, stabilizes ribonucleoprotein particles (114, 72, 73, 8), which enabled workers to purify and preserve ribosomes for physical studies.

In 1959, Tissières, Watson, Schlessinger and Hollingworth (137) confirmed the stabilizing role of magnesium on ribosomes of Escherichia coli and outlined a method of preparation and purification of ribosomal particles. They found that in suitable concentrations of magnesium, four kinds of ribonucleoprotein particles from E. coli were observed with sedimentation coefficients of approximately 30S, 50S, 70S, and 100S with molecular weights of about 1.0, 1.8, 3.1, and 5.9 x 10^6 daltons, respectively.

Since 1959, ribosomes from many sources and especially those from E. coli have been extensively studied, giving insight to the physical structure and the function of these complex ribonucleoprotein particles. The clearly established function of the ribosomes is that they are centrally involved in protein synthesis. (For a review, see 70, 95.) Factors and conditions necessary for protein synthesis have been well established, but little is known about the actual mechanism involved. The understanding of the mechanism of protein synthesis is closely associated with the understanding of the structure and function of the ribosome. In spite of the numerous studies over the past decade, the actual configuration of the ribosome is still virtually unknown. However, a brief review of contemporary knowledge of the structure of the ribosome may be of value in determining what information can or should be sought.

Electron Microscopy of Ribosomes

Some of the first attempts to obtain the size and shape of ribosomes involved electron microscopy. The ribosomes of E. coli were studied using metal shadowing by Hall and Slayter (40), using positive and negative staining by Huxley and Zubay (51), and using metal shadowing and negative staining by Spirin, Kiselev, Shakulov, and Bogdanov (122). Although the results of these air-dried particles varied, a general picture of the ribosomal particles was given. The 100S particle was found to be a dimer of 70S particles attached through their 30S subunits with dimensions of 140-150 x 400 Å (51, 122). The 70S particle had dimensions of 150-170 x 190-200 Å; the 50S particle, 140 x 170 Å; and the 30S particle was found to be a flattened sphere with dimensions of 70-95 x 140-180 Å (40, 51, 122). Slightly larger volumes for the 50S subunit were found by Hart (42,43) using frozen-dried, tungsten-shadowed particles which gave dimensions of 160 x 230 Å. A more recent study by Vasiliev (145) on 70S particles using the frozen-dried, shadowing technique has shown these particles to have a 25% greater volume than air dried (40) or negatively contrasted (51, 12) ribosomes. Vasiliev found the dimensions to be 260-240 Å x 240-220 Å x 180-160 Å, giving an elliptical shape of roughly 1:1.35:1.5. He found the 50S to be typically domed shaped with no large surface grooves as postulated by Bruskov and Kiselev (12). He found the 30S to have a convex-concave

form with a groove running down the long dimension. This study and the previous ones mentioned indicate that the 30S subunit appears to sit as a cap on the 50S subunit to form the 70S particle.

In addition to these determinations, other probable structural features were observed. There was no evidence for a protein shell as in virus particles nor was there any extensive localization of RNA (51). There were, however, surface features observed (43, 145) that did indicate packing of ribonucleoprotein strands with a mean diameter of 30 Å.

Another technique which utilizes optical diffraction analysis of electron micrographs for three dimensional structural studies on ribonucleoprotein particles has been developed by Lake and Slayter (68). They found that in the closely packed helices of ribonucleoprotein particles found in chromatoid bodies of cysts of Entamoeba invadens, the dimensions of the asymmetric unit corresponded reasonably well with those dimensions given by Hill, Thompson, and Anderegg (46) from small-angle x-ray scattering for the 70S E. coli ribosomes. Although the asymmetric unit of the helix has not been shown to be a ribosome, the comparison with the ribosome may be valid.

There has been no single crystal x-ray diffraction work on ribosomes. Byers (14) and Mottet and Hammer (92) have isolated ribosome tetramers in embryonic chick cells.

Crystals that may be large enough for x-ray diffraction analysis have been isolated by Barbieri et al. (3).

There have been studies on the x-ray scattering from gels of ribosomes or ribosomal subunits. Early work on E. coli ribosomes (60, 69, 154) indicated that wet gel patterns have many of the same reflections as those observed with ribosomal RNA (rRNA) while the dry samples had protein-like diffraction patterns. These studies (60, 154) indicated the observed scattering resembles that due to a mixture of protein and rRNA.

Small-angle X-ray Scattering of Ribosomes

X-ray scattering from solutions of ribosomes has been done on the 80S ribosomes of rabbit reticulocytes (23) and beef pancreas (7) and more recently on the 70S (46, 59), the 50S (46, 59, 119) and on the 30S (46, 120) particles of E. coli. The studies by Hill et. al. (46) found the radii of gyration to be 125, 77, and 69 Å for the 70, 50, and 30S ribosome, respectively. The 70S was found to be the shape of an elliptical cylinder with dimensions of 135 x 200 x 400 Å; the 50S, an ellipsoid of 130 x 170 x 310 Å; the 30S, an oblate ellipsoid of about 55 x 220 x 220 Å (46, 120). In agreement with electron microscopy studies, the x-ray scattering studies have not shown a central core of RNA or protein (46, 120), although there is some evidence to the contrary (119). However, the x-ray studies on solutions have indicated volumes consid-

erably greater than those found in electron microscopy, except for the electron microscope studies on frozen-dried samples (43, 145). The long dimension (400 Å) of the 70S ribosome is approximately twice the dimension found with the electron microscope. The 50S particle has dimensions that are about 30% larger, and the 30S particle has a diameter 20% larger. This discrepancy might be attributed to shrinkage incurred in the preparation of the air-dried samples for the electron microscope. Overall, the x-ray scattering from solutions seems to give a more appropriate characterization of ribosomes in their native state than the techniques utilizing dried particles.

Hydrodynamic Properties of Ribosomes

Various other physical parameters have been measured for *E. coli* ribosomes. As mentioned previously, Tissières *et al.* (137) obtained molecular weights, using sedimentation and diffusion coefficients and sedimentation and viscosity. More recently, Hill, Rossetti and Van Holde (45) measured the molecular weights by sedimentation equilibrium and obtained values of 2.65×10^6, 1.55×10^6, and 0.90×10^6 daltons for the 70S, 50S, and 30S particles respectively. Similar results were also obtained with light scattering (112). Sedimentation (45, 137) and diffusion coefficients (137), intrinsic viscosity (45, 137) and partial specific volumes (45, 137) have also been measured for *E. coli* ribosomes.

One of the problems which complicates the study of E. coli ribosomes arises from the fact that different researchers have used a variety of ways to isolate and purify these particles. There are basically three purification techniques that have been widely used. In one technique ribosomes are prepared in Tris- or phosphate buffer containing 0.01 M $MgCl_2$ (137). In another 0.5 or 1 M NH_4Cl is used to "wash" the particles free of nonribosomal protein (112, 128). In the other purification method various concentrations of ammonium sulfate are used to differentially precipitate the ribosomes (63). Hill, Anderegg, and Van Holde (44) found that the unwashed ribosomal subunits contained approximately 10^5 daltons more material than the subunits prepared by the NH_4Cl or the $(NH_4)_2SO_4$ method. The loss of material is presumably protein as $(NH_4)_2SO_4$ precipitated ribosomes contain about 30-33% protein (63), while unwashed ribosomes contain about 37% protein (137). Thus, the interpretation of physical parameters obtained by various workers can be complicated due to the method of ribosome preparation.

Ribosomal RNA

Other studies have yielded information about the ribosome through analysis of the RNA and protein components. As noted above, ribosomal RNA accounts for 60-70% of the mass of the ribosome. The 30S ribosomal subunit contains one molecule of 16S rRNA of about 1700 nucleotides with a

molecular weight of 6.4×10^5 (98), whereas the 50S subunit contains one molecule of 23S rRNA of about 3100 nucleotides with a molecular weight of 1.1×10^6 and one molecule of 5S rRNA of 120 nucleotides with a molecular weight of 4×10^4 (11, 62, 85, 127). The base sequence of the 16S and 23S rRNA is not known, but serious attempts are being made to sequence them (30, 31).

Ribosomal RNA is believed to have a secondary structure of which the rRNA contains many regions in which the single chain doubles back upon itself forming hairpin loop double-stranded helices connected by flexible single-stranded regions (24). The rRNA is 60-70% base paired (13, 80, 111) and is believed to be similar to the secondary structure of the rRNA in the ribosomal subunits (155, 60, 84, 115, 134). The tertiary structure, however, does not seem to be the same in isolated rRNA and in the ribosome as rRNA itself occupies a greater volume than the complete ribosomal subunit (120, 84).

Ribosomal Proteins

The protein complement of the ribosome was found to be heterogeneous in 1960 by Waller and Harris (147). However, studies on the ribosomal protein lagged far behind studies on rRNA. It was not until 1964 that serious studies on the structure of *E. coli* ribosomes were made. As a result of these studies, it has been found that ribosomes consist of

many different proteins in addition to the rRNA. The 30S subunit contains 21 different proteins which have now been isolated and characterized (142, 56, 89, 33, 41, 20, 141, 96, 58, 26, 57, 130, 55, 48, 151, 146), and the 50S subunit contains approximately 35 proteins (26, 57, 47, 90), two (L7-L12) of which may be the same.

The 30S subunit contains approximately 260,000 to 280,000 daltons of protein (20, 41), and the number average molecular weight of an individual ribosomal protein is in the neighborhood of 20,000 daltons (87). However, the aggregate mass of all the proteins on the 30S subunit is about 440,000 daltons (146), considerably greater than the 260-280,000 daltons observed. This discrepancy has been taken to imply that 30S subunits are heterogenous in the protein complement. Futher studies have indicated that there may be 5 to 9 proteins which are not always present (fractional proteins), and 6 to 12 proteins which are always present (unit proteins) (146).

The heterogeneity of the ribosomal subunit has led to the postulation that there are different classes of ribosomes with different functions. Another proposal to explain the heterogeneity is that there is an exchange of fractional proteins to facilitate specific steps of protein synthesis. Evidence for the latter has been shown by Duin, Knippenberg, Dieben, and Kurland (25). They found that the absence of protein S21 enhances the binding of formylmethionyl

transfer RNA and suggested that S21 must be absent from a ribosome which is chain initiating.

The protein complement of the 50S subunit is also heterogeneous. Dizionara, Kaltschmidt, and Wittmann (26) have shown the aggregate mass of the proteins to be about 550,000 daltons having a range of 7,500 to 50,000 daltons. Studies by Weber (148) have shown that the 50S particle has 9-10 "fractional" proteins, 15-16 "unit" proteins, one "repeated" protein of approximately 2 copies per 50S particle, and 7 "fractional repeated" proteins of approximately 1.5 copies per 50S particle.

Ribosomal Precursor Particles

The study of structural transformations in ribosomes and ribosomal subunits has also been used to gather information on ribosomes. Experiments have been performed to learn the sequence of biochemical events occuring in the ribosome assembly process. These experiments have sought precursor particles by the kinetic analysis of RNA precursors, by the use of metabolic inhibitors to cause accumulation of intermediate particles, and by the use of defective mutants of steps in the assembly process. These various experiments have shown slightly different precursor particles but overall have shown ribosome assembly to be a stepwise process. The biogenesis of the 30S subunit seems to start with 16S rRNA and goes via 21S and 26S intermediates to form the 30S

ribosomal subunit (66, 99, 39, 77). The 50S subunit seems to start with 23S rRNA and goes via 32S and 43S intermediates to form the 50S ribosomal subunit (39, 77, 100, 22). As of yet, these intermediate particles have yielded little information about the structures of the ribosomal subunits.

Unfolded Ribosomal Particles

In vitro studies have shown that altering the environment of ribosomes and ribosomal subunits can also cause structural transformation in the particles. In 1963, Spirin and coworkers showed electron micrographs of elongated strands resulting from ribosome exposure to high salt followed by exposure to buffer of low ionic strength containing no magnesium (122). Exposure to high salt, low magnesium, or direct removal of divalent cations by chelation gives rise to altered ribosomal particles (15, 35, 36, 78, 94, 108, 133, 149, 150, 44). Similar affects have also been accomplished by heating (134, 6, 135). These particles have decreased sedimentation coefficients and increased intrinsic viscosity (134, 150, 123) which is due to a loosening of the ribonucleoprotein strand. However, the structural alteration does not seem to be due to a general loosening that would give many differently shaped particles, as the denaturation occurs in discrete intermediate steps that can be summarized as follows:

$$50S \rightarrow 40S \rightarrow 30S \rightarrow 19S$$

$$30S \rightarrow 27S \rightarrow 23S$$

Analysis by electron microscopy (122, 80, 70) and optical rotatory dispersion (135, 29), has indicated that the loosening process seems to be due to an unfolding of particular portions of the particle.

Upon unfolding the 50S subunit one step, 85 to 90% of the 5S rRNA and 4 to 7 proteins are released (38). Proteins on the unfolded 30S particles, however, seem to remain associated with the RNA (134, 140, 36). One of the major problems in the study of these intermediate particles is that of isolating homogeneous samples. Although the 39S and 30S unfolded particles have been isolated and partially characterized (44, 79), no homogeneous intermediate(s) has been isolated for the 30S subunit.

While the results from these studies are slightly ambiguous, they have indicated that the ribosomal subunits are composed of a folded ribonucleoprotein strand. Small-angle x-ray scattering from the 23S particle (120) has also shown that the 30S subunit appears to expand in one dimension while the small dimension remains fairly constant. This evidence is consistent with the idea that the subunit is composed of a folded strand.

To help visualize this phenomenon of unfolding in one dimension, a useful analogy is to compare the RNP

strand to a piece of rope laying on a table. The rope is folded into non-overlapping, "hairpin-type" loops, forming an overall shape of a square. The square actually has three dimensions, as the depth is the diameter of the rope. If a free end of the rope is pulled in a direction perpendicular to the folds, one observes three obvious effects. First, the shape approximated by the folded strand is now a rectangle, as one dimension of the square has been lengthened. Second, the loops of the rope have been loosened or unfolded. Third, the small dimension as determined by the thickness of the rope has remained constant.

Protein-deficient Particles

Another method to obtain altered ribosomal particles is the selective removal of proteins from the subunits. Exposing the ribosomal subunits to high salt, concentrations of 1-2 M when magnesium is no more than 0.01 M, causes a loss of protein giving protein-deficient ribosomal particles, or core particles. The technique of stripping proteins from subunits by means of high concentrations of CsCl was discovered by Meselson et al. (83), and similar dissociation of protein from subunits was found to occur when exposed to LiCl (2, 52), KCl, or NH_4Cl (121) in high concentration. The proteins thus removed have been separated into acidic and basic fractions (138). The

release of protein was shown to occur stepwise by way of discrete intermediate stages (52, 71), and most interestingly, the 23S core particle would reassociate with the dissociated protein under the proper conditions to yield functionally active subunits (71, 49, 125). Although studies of protein-deficient particles have the potential of offering much information about the tertiary folding of the RNA-protein strand and the factors responsible, little work has been done. Smith (120) has shown the 23S core particle to have a greater maximum dimension than the 30S subunit. The expansion of this protein-deficient particle was taken as evidence that the proteins contributed to maintaining the compact structure of the 30S subunit.

Reconstitution of Ribosomes

The spontaneous assembly of the 30S subunit from core particles and dissociated proteins led to the *in vitro* method developed by Traub and Nomura (139) of reconstituting functionally active 30S subunits from the ribosomal proteins and rRNA. This method was used to look closely at the mechanism of assembly for the 30S subunit (140, 86, 97). It was determined that reconstitution requires the use of a rather high ionic strength solution, the optimal ionic strength being 0.37. In the appropriate ionic conditions, about 12 or 13 proteins combine with rRNA to form a reconstitution intermediate, RI. At this

point the rate-limiting unimolecular reaction, representing a structural rearrangement of the intermediate with a high activation energy, will occur if heat is supplied by raising the temperature of the incubation mixture to 40° C for 20 minutes. The activated intermediate will then bind the remaining proteins, yielding functional 30S particles with the same shape and internal structure as natural subunits (120). It was found that the proteins bind in a particular order, the "internal" ones binding first, and that several proteins bind to specific sites (86, 116, 129, 118, 117, 34). The implication of specific interdependence of protein-protein or protein-RNA interactions suggests a highly specific topographical relationship among ribosomal components in the three-dimensional ribosome structure.

Chemical Modification of Ribosomal Proteins

This implied topographical relationship of ribosomal components has led to the study of the structure of the ribosome by chemical methods. Various protein reagents have been used as chemical probes to determine the relative "internal" or "external" position of the ribosomal proteins. Iodoacetate (19), N-ethyl maleimide (88), 2-methoxy-5-nitropropone (19), trypsin (19, 16, 21), fluorescein isothiocyanate (50), and gluteraldehyde (54) are among the reagents that have been used. Chemical modification studies, while relatively straightforward experimentally, often seem

to be difficult to interpret unequivocally due to the degree of accessibility of both the protein and the reacting groups within the protein. This may be one of the reasons why the agreement among these data is not good.

Stöffler et al. (131) have shown that every one of the 30S proteins within intact subunits have antigenic sites available for interaction with its specific antibody. This data implies that all 30S proteins are exposed to the external milieu to a certain degree. Therefore, the use of chemical modification of the proteins to determine the relative "internal" or "external" position of the proteins may be in vain. This technique may be useful, however, to determine whether or not certain proteins are buried in the 70S ribosome (50).

Nuclease Derived Ribonucleoprotein Fragments

Another method to probe the structure of the ribosome involves mild degradation of the ribosomal subunit by nucleases. Several investigators have described conditions that have shown that controlled nuclease digestion produces large subparticles from both 50S and 30S ribosomes (1, 27, 32, 9, 10, 37, 110, 114). One conclusion developed in these experiments is that the three-dimensional structure of the native ribosomes influences the susceptibility of the RNA to enzymatic attack. If this conclusion is correct, then the products of the nuclease digestion

should reflect gross features of the three-dimensional structure of the ribosome. Thus, an analysis of the protein compositions of the particles released by nuclease action might give some clues to the three-dimensional arrangement of the proteins. Brimacombe, Morgan, Oakley, and Cox (9, 10) have isolated fragments from the 30S subunit and found that they contained different proteins. Schendel, Maeba, and Craven (114) have also used nuclease to isolate three subparticles from the 30S subunit. The proteins on the fragments were identified and each of the 21 proteins appeared to be a component of at least one of the three particles. They have also shown that comparison of the distribution of the proteins with their sequence of assembly suggests that those proteins that are directly interdependent in the assembly reaction are associated on the same subparticles. The subparticles isolated were thought to be unbroken lengths of unfolded RNA associated with those proteins that interact with the RNA. The subparticles were found to have proteins common to each other and were interpreted as being overlapping fragments. From this viewpoint, they were able to postulate a sequence of proteins existing in the native 30S subunit.

Morgan and Brimacombe (91) and Roth and Nierhaus (109) have used nuclease digestion to obtain a number of ribonucleoprotein particles. The individual proteins found

in specific fragments were interpreted as being close neighbors in the 30S particle. Unlike Schendel *et al.* (114), these workers did not try to postulate a linear sequence of proteins, but they incorporated their data into a rearranged version of the "assembly map."

While the nuclease digestion method appears to be a valid method for the determinations of specific groups of proteins, it appears premature to apply these results to a linear arrangement of the proteins along the rRNA. The structure of the rRNA may be such that although the proteins are neighbors on a specific RNP fragment, this fragment, when incorporated into the intact 30S particle, may be folded in such a way that the proteins are no longer close neighbors. Thus, a linear sequence of the proteins may not have any importance in the determination of the ribosome structure. However, when such a sequence is applied to the assembly relationship of the 30S subunit, quite possibly much information about the three-dimensional organization of the proteins and thus the ribosome itself will be gained.

Research Proposal

In summary, studies to date have shown gross features of the ribosome. The proteins have been characterized and identified for both the 50 and 30S subunits but more completely for the 30S particle. Partial character-

ization of unfolded particles has been done, but only the 39S and 16S particles have been studied using homogeneous samples. Partial reconstitution of the 50S subunit has been done, but total reconstitution of the 30S particle has been shown. Because of the reconstitution experiment, it is felt that more is known concerning the structure of the 30S subunit, and correspondingly, the information of the three-dimensional structure would be easier to obtain. For these reasons, a study to gain insight of the structure of the 30S subunit was undertaken.

To obtain information of the tertiary folding of the ribonucleoprotein strand of the 30S ribosome, it was decided to obtain the unfolded 30S particle, namely the 23S particle. Although studies have been made on solutions containing this and other particles, it was felt that physical studies of homogeneous 23S particles would lead to a more detailed interpretation of the tertiary folding. Thus, it was necessary to develop the techniques and conditions needed to obtain this particle. The 23S particle was then characterized with sedimentation velocity and equilibrium studies and viscosity measurements.

Since the unfolding appears to take place in discrete steps, it is felt that this process is due to unfolding of particular portions of the subunit. If this is true, it was felt that a physical shearing of the extended portion(s) would be possible. To accomplish this, the 23S particle

was subjected to sonication that resulted in two major particles having lower sedimentation coefficients. The particles were then separated and the protein components of each identified by means of acrylamide gel electrophoresis. In addition to postulating a model to fit the results obtained, these data were compared to protein sequence data previously found by other workers.

CHAPTER II

PREPARATIVE PROCEDURES

Bacteria

Escherichia coli, strain MRE 600, which has an inactive Ribonuclease I, was used as the source of ribosomes. The media used to grow the bacteria was as follows:

$(NH_4)_2SO_4$	0.4 g/liter
Na_2HPO_4	7.5 g/liter
KH_2PO_4	9.8 g/liter
$Na_3Citrate \cdot 2H_2O$	0.4 g/liter
$MgCl_2$	0.042 g/liter
$CaCl_2$	0.010 g/liter
$Fe(NH_4)_2(SO_4)_2$	0.015 g/liter
glucose	10 g/liter
yeast extract	5 g/liter

The cells were grown until the culture had an optical density of 2 OD units at 650 nm. At this time the cells were iced and harvested. The bacteria were obtained through the auspices of Dr. James Young and stored at -74° C until ready for use.

65S Ribosomes

The 65S ribosomes were prepared by a method similar to that described by Hill et al. (45). About 100 g of bacteria were washed twice in 250 ml of buffer (0.015 M $MgCl_2$, 0.5 M NH_4Cl, 0.01 M Tris-HCl, pH 7.4) (65S buffer) and then mixed with 50 ml of 120 μ glass beads and ground for 30 minutes at 22,000 rev/min in a Gifford-Wood Mini Mill set at a 0.03" spacing. This suspension was then mixed with 200 ml of 65S buffer and centrifuged in a Beckman J-21 preparative centrifuge with a JA-20 rotor at 10,000 rev/ min (12,000xg) for 10 minutes to remove the glass beads and large cellular debris. The resultant supernatant was spun at 48,000xg for 45 min. to further clarify the solution. The supernatant was then decanted and spun in a type 60 Ti rotor in a Beckman L2-65B ultracentrifuge at 60,000 rev/min (361,000xg) for 2 hours to pellet the ribosomes. These pellets were then resuspended in 90 ml of 65S buffer and stirred overnight (16 hours) to wash the ribosomes of any residual ribonuclease (126) and nonribosomal protein (63). On some preparations this wash time was shortened to 6 hours. Following the wash, the ribosome solution was clarified by centrifugation at 48,000xg for 45 minutes, and the ribosomes were then pelleted by centrifugation in a type 65 rotor at 65,000 rev/min (368,000xg) for 75 minutes. These were then used to obtain 30S subunits.

30S Ribosomal Subunits

The 65S ribosome pellets were resuspended in about 35 ml of buffer (0.001 m $MgCl_2$, 0.1 M KCl, 0.01 M Tris-HCl, pH 7.4) (30/50 buffer) and stirred for 3 hours to dissociate the ribosomes into 30S and 50S subunits. These subunits were then separated by zonal ultracentrifugation using a technique similar to that of Eikenberry, Bickle, Traut, and Price (28) as follows: A 10 to 30 percent linear sucrose gradient in 30/50 buffer was generated in a Beckman type Ti-15 rotor with a B-29 insert by producing a 10 to 30% exponential gradient formed by using 800 ml of 36.9% (w/w) sucrose in the moving chamber and 550 ml of 10% (w/w) sucrose in the fixed, mixing chamber of an International Equipment Company Gradient Pump. The gradient was pumped at a rate of 30 ml/min into the outside edge of the rotor, followed by a cushion of 550 ml of 50% (w/w) sucrose to fill the rotor. All loading and unloading of the rotor was done at 4 to 8° C with the rotor spinning at 3,000 rev/min. Approximately 70 ml of sample, containing 1 to 2 g of 30S and 50S subunits in an inverse gradient of 10 to 0% (w/w) sucrose in 30/50 buffer, was introduced into the center of the rotor followed by 400 ml of a 30/50 buffer overlay. The rotor was spun at 121, 750xg for 9 hours at 4° C. Edge unloading was accomplished by displacing the gradient with water pumped into the center of the rotor at a rate of 30 ml/min. Fractions of 10 ml were collected on a Gilson

Fraction Collector and their absorbance at 260 nm determined on a Cary 15 spectrophotometer. The fractions containing the 30S subunits were then pooled. The profile of a typical elution pattern is shown in Figure 1.

The 30S subunits were recovered from the sucrose with the ethanol precipitation method as described by Staehelin and Maglott (124) in which the Mg^{++} concentration of the pooled fraction was raised 10 fold and 1.5 volumes of cold ethanol was added. The precipitated subunits were then pelleted by centrifugation at 28,000xg for 10 minutes, and the pellets were resuspended in 5 to 10 ml of buffer (0.0015 M $MgCl_2$, 0.07 M KCl, 0.01 M Tris-HCl, pH 7.4) (30S buffer). To remove the remaining sucrose from the solution, dialysis against 30S buffer for 12 hours was necessary. This dialysis was usually done in conjunction with the dialysis needed to obtain the 23S particle. A Schlieren pattern of the purified 30S subunits is given in Figure 2a. These subunits were used immediately or stored at -74° C for future use.

The 23S Particle

Stock solutions of 30S subunits were placed in 1 cm diameter dialysis bags to give a minimum ratio of 1 ml of sample to 200 ml of dialysate. These samples were then dialyzed against 0.0001 M $MgCl_2$, 0.07 M KCl, 0.01 M Tris-HCl, pH 7.4 in deionized, distilled water (23S buffer) for 36 to

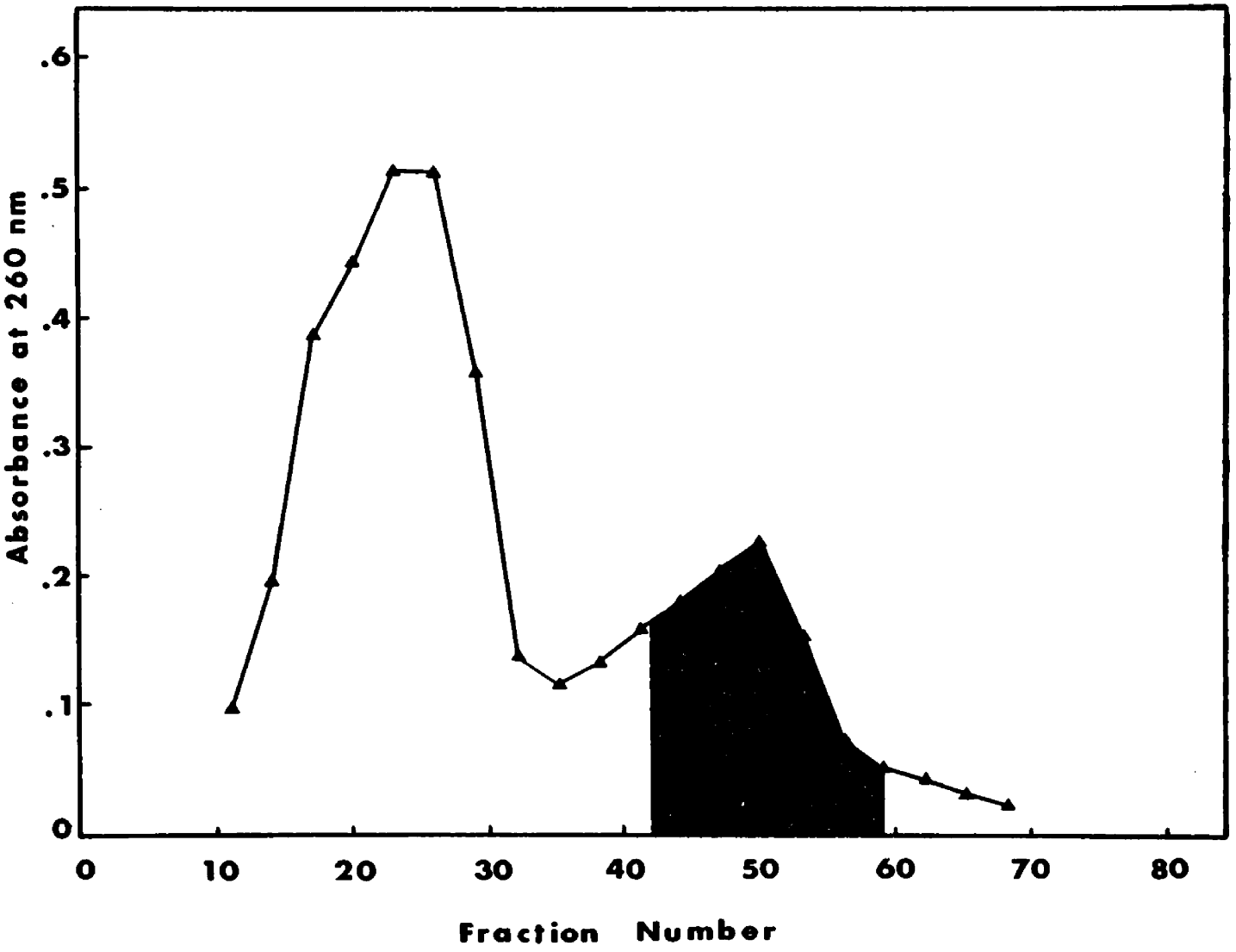

Figure 1. Sucrose gradient elution profile from zonal centrifugation of 30S and 50S ribosomes. The separation of the subunits was done on a 10-30% sucrose gradient in a Ti-15 rotor. The absorbance of 1:100 dilutions of every third tube was read at 260 nm. The shaded area represents the fractions that were pooled for the isolation of 30S subunits.

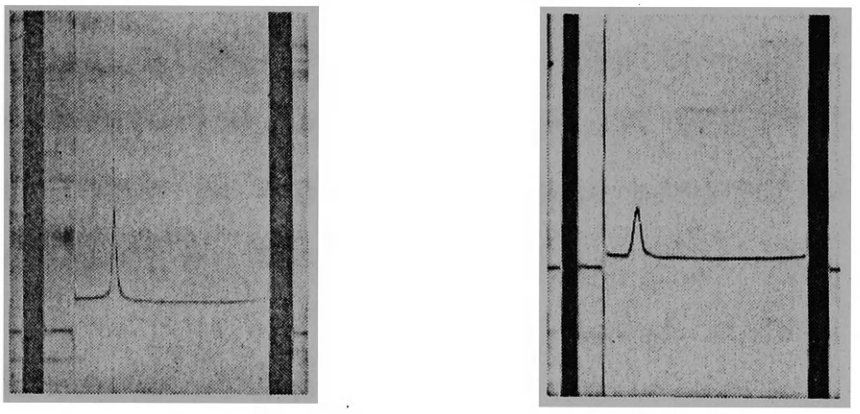

a b

Figure 2. Schlieren patterns of 30S subunits and 23S particles: (a) 30S subunits, (b) 23S particles. Both pictures were taken 12 minutes after reaching a speed of 60,000 rpm, at a temperature of 4° C, and a phase plate angle of 75. Sedimentation is from left to right.

60 hours at 4° C with continual stirring. The dialysate was changed 6 times during this period. The amount of time for dialysis was determined for each individual sample by monitoring the sample with time in the analytical ultracentrifuge using schlieren optics. For most samples, 48 hours of dialysis was sufficient. The resulting particles have a sedimentation coefficient of 23S and give a schlieren pattern as shown in Figure 2b. These samples were then used immediately or stored at -74° C.

Sonicated 23S Particles

Sonication of stock solutions of the 23S particle was done for 20 minutes at the maximum setting on a Bronwill Biosonik III. Five ml of sample was placed in a small glass beaker and kept in a salted-ice bath to minimize temperature effects during sonication. The results of sonication are shown in the schlieren pattern given in Figure 3a.

Zonal centrifugation as previously described to isolate the 30S subunit was used to isolate the particles from the sonicated 23S sample. However, in this case 140 mg of sample was applied to the rotor, and the rotor was spun at 121,750xg for 20 hours. The gradient was collected in 10 ml fractions, and the absorbancy at 280 nm determined for each fraction. The extinction coefficient at 280 nm is approximately one half the extinction coefficient at

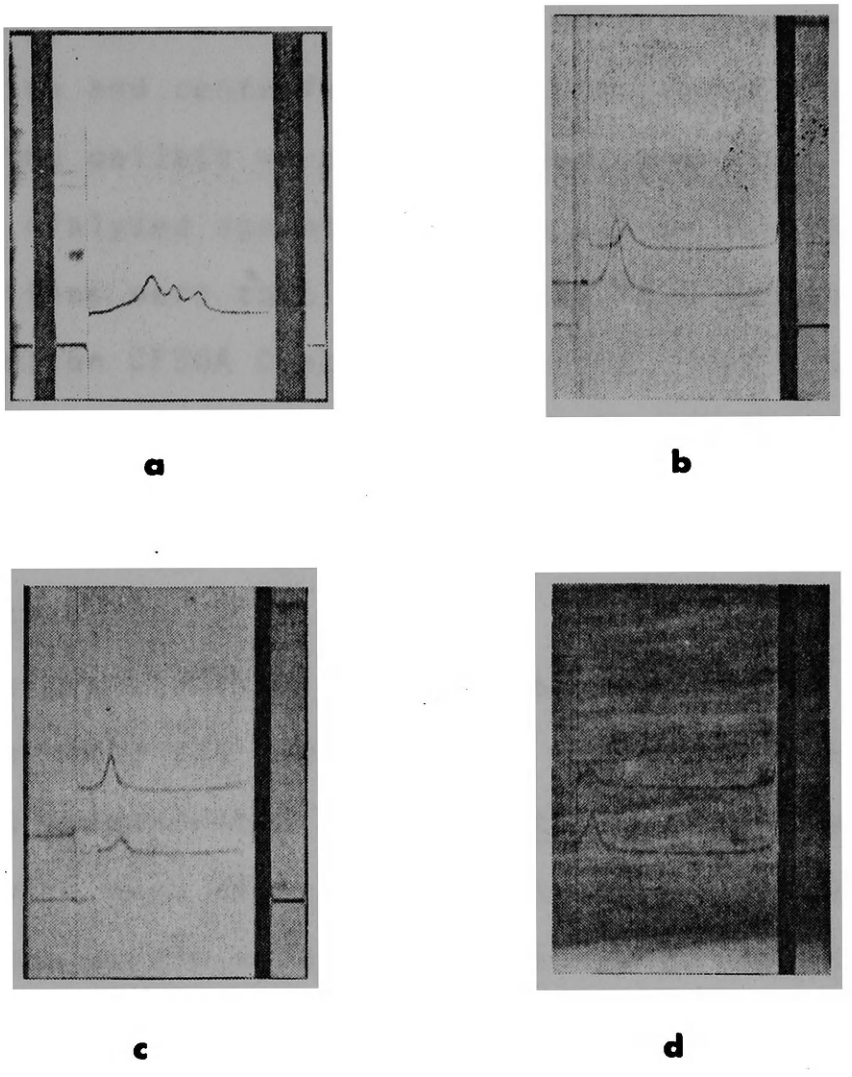

Figure 3. Schlieren patterns of sonicated 23S particles, 23S, 15S, 10S, and 5S sonicated particles: (a) the results of sonication of the 23S particle, and the particles isolated as in figure 11, (b) 15S (upper) and 23S sonicated particles, (c) 15S and 10S sonicated particles, and (d) 5S and 10S sonicated particles. A standard and 1° positive wedge cell were utilized for (b), (c), and (d). The centrifugation was done at 60,000 rpm at 4° C. Sedimentation is from left to right.

260 nm which, in this case, enabled direct absorption determinations of the fractions without any dilution of the fractions. The appropriate fractions under each peak were pooled, and the particles were recovered by ethanol precipitation and centrifugation as previously described. The resulting pellets were resuspended in 5 ml of 23S buffer and dialyzed against the same buffer for 12 hours. These solutions were then concentrated to a volume of 1.5 ml using Amicon CF50A Centriflo membrane cones. Schlieren patterns of these particles are shown in Figures 3b and 3c. These particles were then stored at -74° C.

Protein Extraction

The protein from the 30S subunit, the 23S particle, and the sonicated 23S particles was extracted with 66% acetic acid as described in Hardy et al. (41). The protein solutions were then dialyzed against 6M urea for 12 hours to remove the acetic acid. When necessary, protein solutions were concentrated in an Amicon Model 8MC ultrafiltration cell with a UM-2 membrane.

CHAPTER III

SAMPLE ANALYSIS

Concentration Measurements

Concentration measurements were determined from the optical density measured at 260 nm using $E^{1\%}_{260}$ = 145 for the 30S subunit (45) and the 23S particle and $E^{1\%}_{260}$ = 223 for ribosomal RNA (127). The optical density measurements were made with either a Cary 15 or a Gilford Model 2000 spectrophotometer attached to a Beckman DU.

Protein concentrations were measured by the method of Lowry *et al.* (74), using bovine albumin (Sigma Chemical Co.) as a standard. RNA concentrations were measured by the orcinol method of Mejbaum (82), using 16S rRNA as a standard.

Analytical Ultracentrifugation

Sedimentation velocity experiments to obtain the sedimentation coefficients and to determine sample purity were made on a Spinco Model E analytical ultracentrifuge using schlieren optics. An AN-D rotor with a 12 mm Kel-F centerpiece, 4°, single sector cell with quartz windows was used. When two cells were used, a 1° positive wedge window was used in one cell to displace its image.

Sedimentation coefficients were determined from measurements of the maximum of the schlieren peak on Kodak

Metallographic Plates with a Nikon Profile Projector Model 6C. These data were then analyzed by a program written by myself designed for a Wang 600 which gave the sedimentation coefficient corrected for the viscosity and density of the buffer. Determination of the $s^{\circ}_{20,W}$ value was made by extrapolating the sedimentation coefficients obtained at a series of concentrations corrected for radial dilution to infinite dilution.

Sedimentation equilibrium experiments to determine the molecular weight of the 23S particle was made in the Spinco Model E analytical ultracentrifuge utilizing the high-speed technique developed by Yphantis (152). Solutions of initial concentrations between 0.3 to 0.6 mg/ml were run using a double sector cell with a saphire windows in an An-J rotor at 6,000 rev/min at 4° C for 18 to 24 hours. One channel of the centerpiece was filled with 0.11 ml of dialysate and the other channel filled with 0.10 ml of sample giving column heights of about 3 mm. Rayleigh optics were used in the equilibrium experiments, and the interference patterns were photographed on Kodak II-G spectroscopic plates. Fringe positions were measured by averaging the verticle position of five successive fringes at spacings of 50 to 100 μ using the Nikon microcomparator with a 50X objective. These data were then analyzed by a computer program written by Dr. Robert Dyson which gave number-, weight-, and z-average molecular weights at any point in the solution

column, using a quadratic fit over a preset region around each point to obtain these averages.

Viscosity

Relative viscosities of the 23S particle were measured with an Ubbelohde viscometer having a volume of 10 ml and a solvent flow time of 314 sec at 20° C. All flow times were recorded at 20.000 ± 0.001° C to a precision of ± 0.06 sec. Differences in flow times between dialysate and solution varied from 8 to 60 sec, depending upon the concentration of the sample. The reduced viscosity values η_{sp}/c, were corrected for the partial specific volume $\bar{v}$, and the mass density, ρ, and determined at different concentrations. Sedimentation velocity studies were done to determine the effect of the viscosity measurements on the sample. The intrinsic viscosity, $[\eta]$ was determined by an extrapolation of the η_{sp}/c values to infinite dilution.

Partial Specific Volume

The apparent specific volume (ϕ) for the 23S particle was obtained by use of the relation:

$$\phi = \frac{1}{\rho_o}\left(1 - \frac{\rho - \rho_o}{c}\right)$$

where ρ_o is the density of the dialysate and ρ is the density of the solution and c is the concentration of the 23S particle in g/ml. The densities of the dialysate and the

23S particle solutions were measured with a Digital Density Meter DMA 02C manufactured by Anton Parr in accord with the design of Kratky et al. (61). Each set of measurements were preceded and followed by verification of the calibration constant of the instrument with three salt solutions of density previously determined pycnometrically at the same temperature. The precision of the densities obtained from measurements is $\pm$ 1.5 x 10^{-6} when the temperature is controlled to $\pm$ 0.01° C. The measurements of the solutions for this study were made at 4$\pm$ 0.005° C.

The concentrations of both the dialysate and the ribosome solutions were obtained by weighing 1 to 3 ml of the solutions into stoppered flasks, lyophilizing them, and then drying them in a vacuum oven at 98 to 100° C to constant weight (45). Since no variation of ϕ with concentration was apparent, we concluded that ϕ is equal, within experimental error, to the partial specific volume ($\bar{v}$) of the 23S particle.

Extinction Coefficient

The 1% extinction coefficient for a 1 cm curvette at 260 nm, $E^{1\%}_{260}$, was measured for the 23S particle following the procedure of Hill et al. (45). The concentrations of the solution and dialysate were obtained by weighing 10 ml portions in 25 ml tared volumetric flasks and lyophilizing and drying them at 95 to 100° C in vacuo to constant weight. The optical density of the original solution was obtained on

a Cary 15 recording spectrophotometer in order to determine the extinction coefficient.

Electrophoresis

Discontinuous electrophoresis in polyacrylamide gels at pH 4.5 was used to analyze the protein preparations. The electrophoresis was performed by the modification of the techniques of Hardy et al. (41) described by Voynow and Kurland (146). This method utilizes two different methylene-bisacrylamide concentrations depending on the protein being studied; 0.15% (w/v) was used for "soft" gels, and 0.75% (w/v) for "hard" gels. The soft gels were 9 x 0.5 cm, and the hard gels were 10 x 0.5 cm. The electrophoresis was carried out in a Buchler Polyanalyst Disc Electrophoresis Apparatus. The gels were fixed, stained, and destained as in Hardy et al. (41). It was found that 35 to 70 µg of protein in 0.1 to 0.3 ml was sufficient to give darkly stained bands.

CHAPTER IV

RESULTS

UNFOLDED PARTICLE PREPARATION

30S Subunit Preparation

Quantities of 150 to 300 mg. of 30S subunits were routinely obtained with the zonal centrifugation method. Schlieren patterns of the samples (see Figure 2a) consistently showed a single 30S peak with few noticeable contaminants. Extreme care was taken to insure homogeneous samples with no 50S subunit peak present in the schlieren pattern.

Stable Conditions for the 23S Particle

To obtain homogeneous samples of 23S particles, 30S subunits were dialyzed against different buffers containing various concentrations of NH_4Cl, EDTA, $MgCl_2$, Tris, and KCl. With many of the buffers tried, 2 to 3 distinct peaks were present in the schlieren patterns. However, the buffer containing 0.0001 M $MgCl_2$, 0.07 M KCl, 0.01 M Tris-HCl, pH 7.4, gave homogeneous 23S particles upon extended dialysis. The amount of time for dialysis was found to be a critical factor in obtaining the 23S particles. Dialysis for less than 30 to 40 hours gave samples of 23S particles with an additional peak intermediate to 23S and 30S in the schlieren patterns. It was assumed that this peak represented the 27S

particle or was due to a conformational equilibrium between 23S and 30S particles. With additional dialysis, homogeneous samples were obtained giving a schlieren pattern as shown in Figure 1b. As noted in Chapter III, the minimum time for dialysis varied with individual samples. However, these particles appeared to be quite stable as additional dialysis for 20 to 30 hours did not change the schlieren pattern.

PHYSICAL PROPERTIES OF THE 23S PARTICLE

Sedimentation Velocity Studies

Sedimentation coefficients of the 23S particle were measured for each concentration in a dilution series, and the corrected $s_{20,w}$ values were then plotted against the corrected concentrations and extrapolated to infinite dilution. The results, shown in Figure 4, gave an $s^{o}_{20,w} = 23.3 \pm .2$ and were found to fit the relation $s^{o}_{20,w} = (23.3 - .8\ c)$ S, where c is measured in mg./ml. The schlieren patterns showed homogeneous, symmetrical peaks with no mass accumulation near the meniscus.

Partial Specific Volume

The accuracy of a molecular weight determination by sedimentation equilibrium is dependent on the accuracy of the partial specific volume ($\bar{v}$). The measurements of $\bar{v}$ are dependent on the accuracy of the density measurements which were obtained at a precision of $\pm$ 1.5 x 10^{-6}. Therefore,

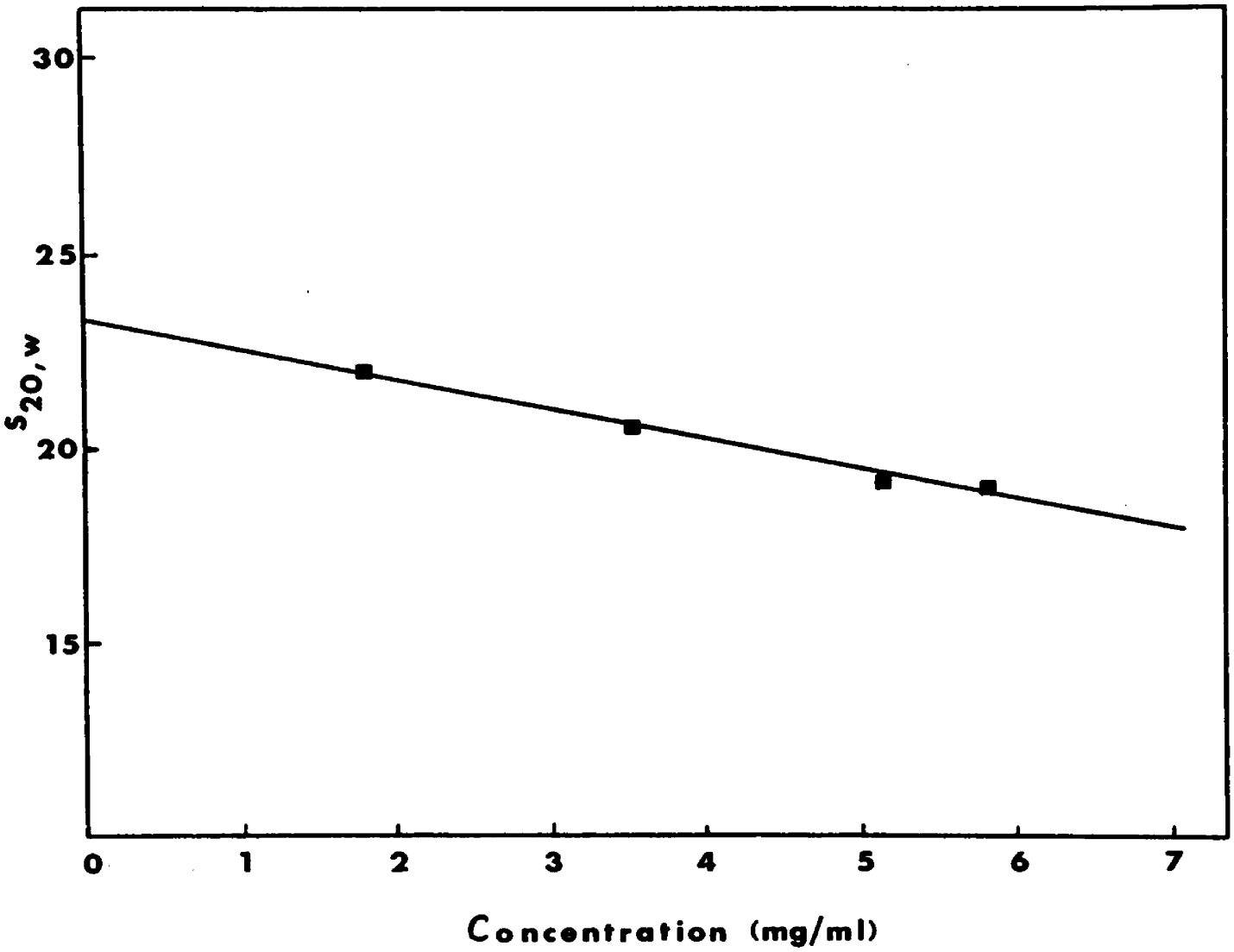

Figure 4. An extrapolation to infinite dilution of the sedimentation coefficients found for the 23S particle. The values were corrected for radial dilution and were obtained at a speed of 60,000 rpm at 4° C with a phase plate angle of 75.

the method employed offers very good precision for the determination of $\bar{v}$. This value is also dependent upon the concentration measurements which were obtained to a precision of ± 0.1%.

The value of $\bar{v}$ was obtained using the densities and concentrations of four ribosome solutions and two dialysate solutions. A plot of solution densities versus concentration, as shown in Figure 5, gives a slope equal to $\frac{\rho - \rho_o}{c}$. The value for the partial specific volume was then calculated as described in Chapter III. We determined the partial specific volume of 23S ribosomal particles to be 0.619 ± 0.006 ml/g at 4° C.

Viscosity Measurements

The corrected reduced viscosity values, $\frac{\eta_{sp}}{c}$, were obtained at a series of dilutions for two samples and plotted against the concentration and extrapolated to infinite dilution. The results, shown in Figure 6, give an intrinsic viscosity value of $[\eta]$ = 11.0 ± 0.2 ml/g.

Extinction Coefficient

No significant change in the extinction coefficient ($E_{260}^{1\%}$) was observed for the subunits unfolded in the low Mg^{++} buffer. The $E_{260}^{1\%}$ of 145 as measured for the 30S subunit (45) was used for UV absorption determinations of concentration.

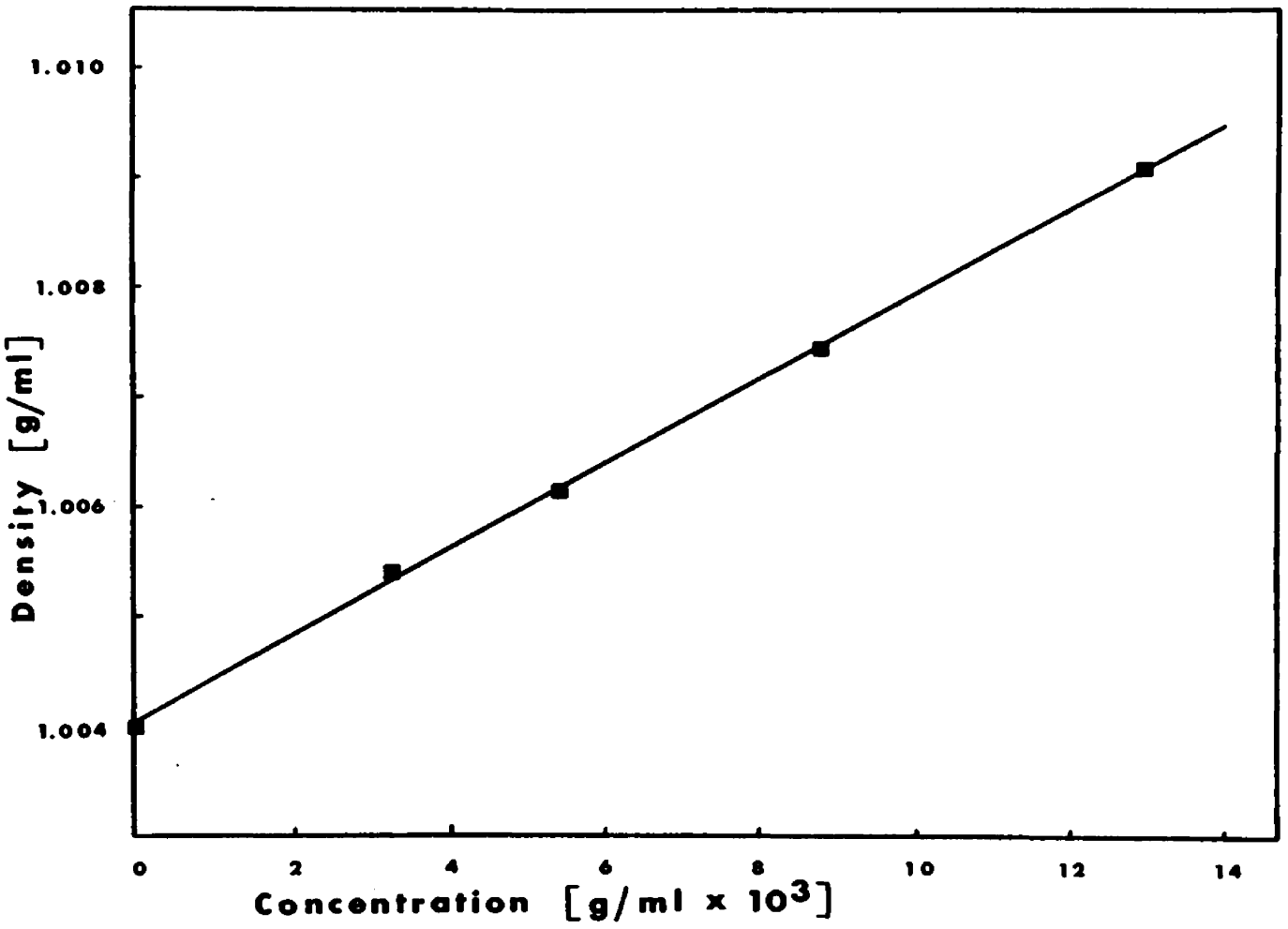

Figure 5. A graph of solution density versus concentration for the 23S particle. The densities were determined with a Precision Density Meter DMA 02C at 4° C.

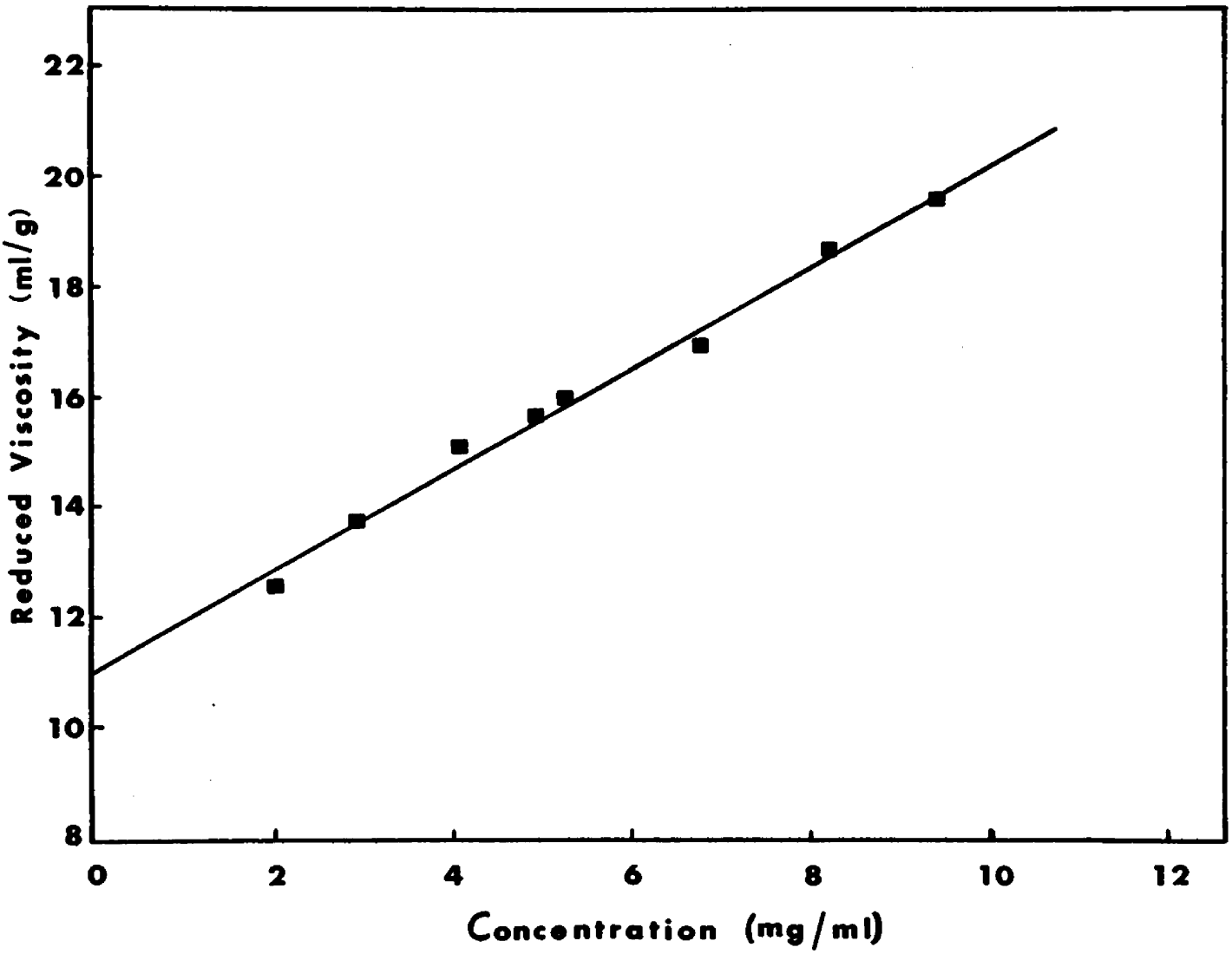

Figure 6. An extrapolation to infinite dilution of the reduced viscosity values for the 23S particle. All values were obtained at 20° C.

Molecular Weight

Obtaining the molecular weight of the 23S particle by sedimentation equilibrium has proven to be difficult. The analysis of the data utilized the method of the calculation of point-average molecular weights across the solution column. This type of analysis gives a clear indication of heterogeneity and/or non-ideality. Figure 8 illustrates the results from one typical sedimentation equilibrium run. The heterogeneity of this sample is clearly evident. The point-average molecular weights are not within experimental error, and the number- and weight-average molecular weights increase across the solution column. A plot of the values of ln j *versus* Δr^2 for this equilibrium run, as shown in Figure 7, also shows the extreme amount of heterogeneity of the sample. For homogeneous, ideal solutions, one obtains a straight line from such a plot.

The fact that the equilibrium runs where heterogeneous was disturbing. The sedimentation velocity studies gave schlieren patterns of single symmetrical peaks. Therefore, it was assumed that there was no more than 5% contaminant of any of the samples. It was originally thought that the contaminating species was protein. To eliminate the protein, samples were centrifuged in sucrose for a period of time that would pellet the 23S particle, but not any contaminating protein. The samples were also eluted on a Sephadex G-100 column to separate protein from the sample.

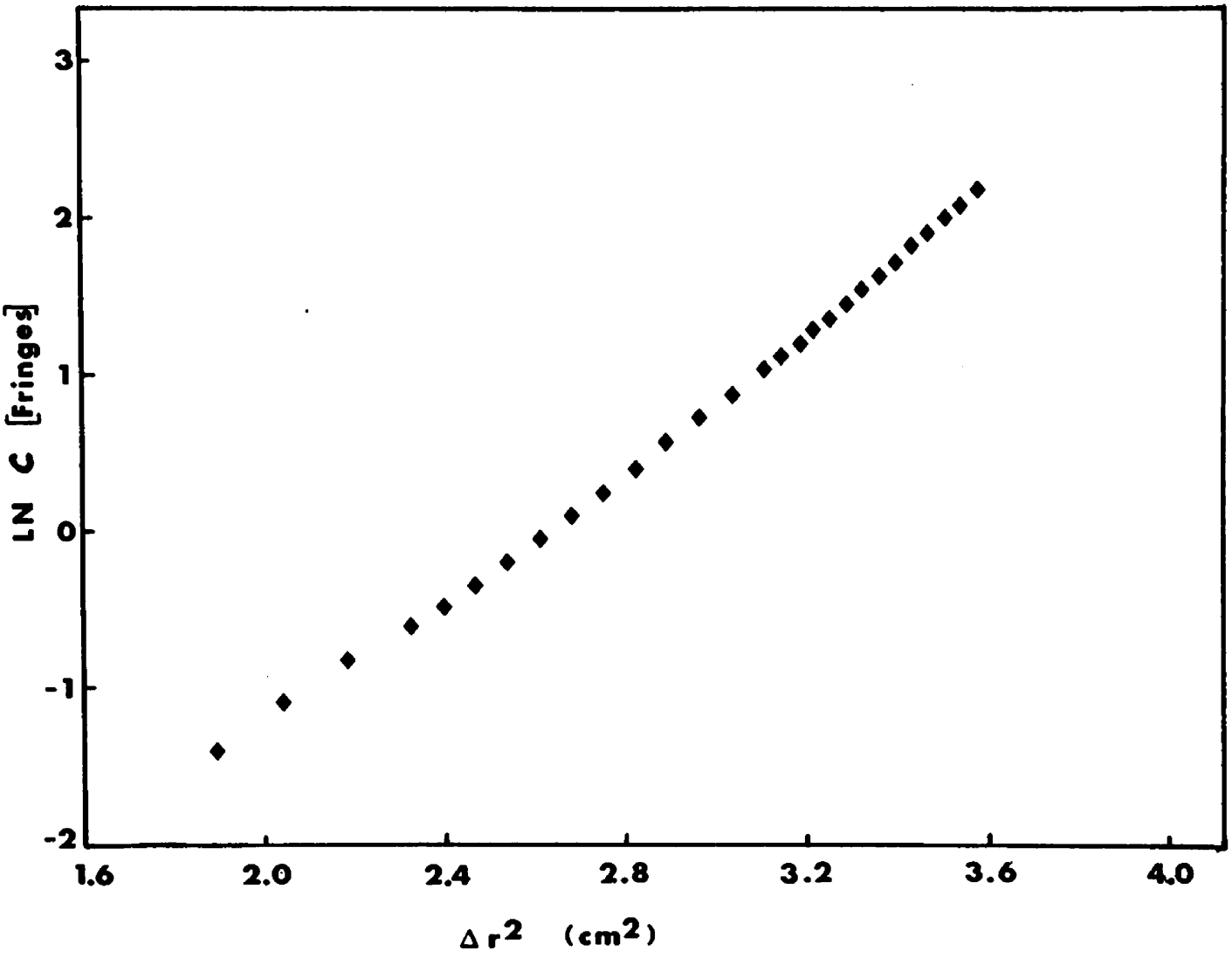

Figure 7. A graph of ln C versus Δr^2 from the sedimentation equilibrium data of the 235 particle. The sedimentation equilibrium was done at 6,400 rpm at 4° C.

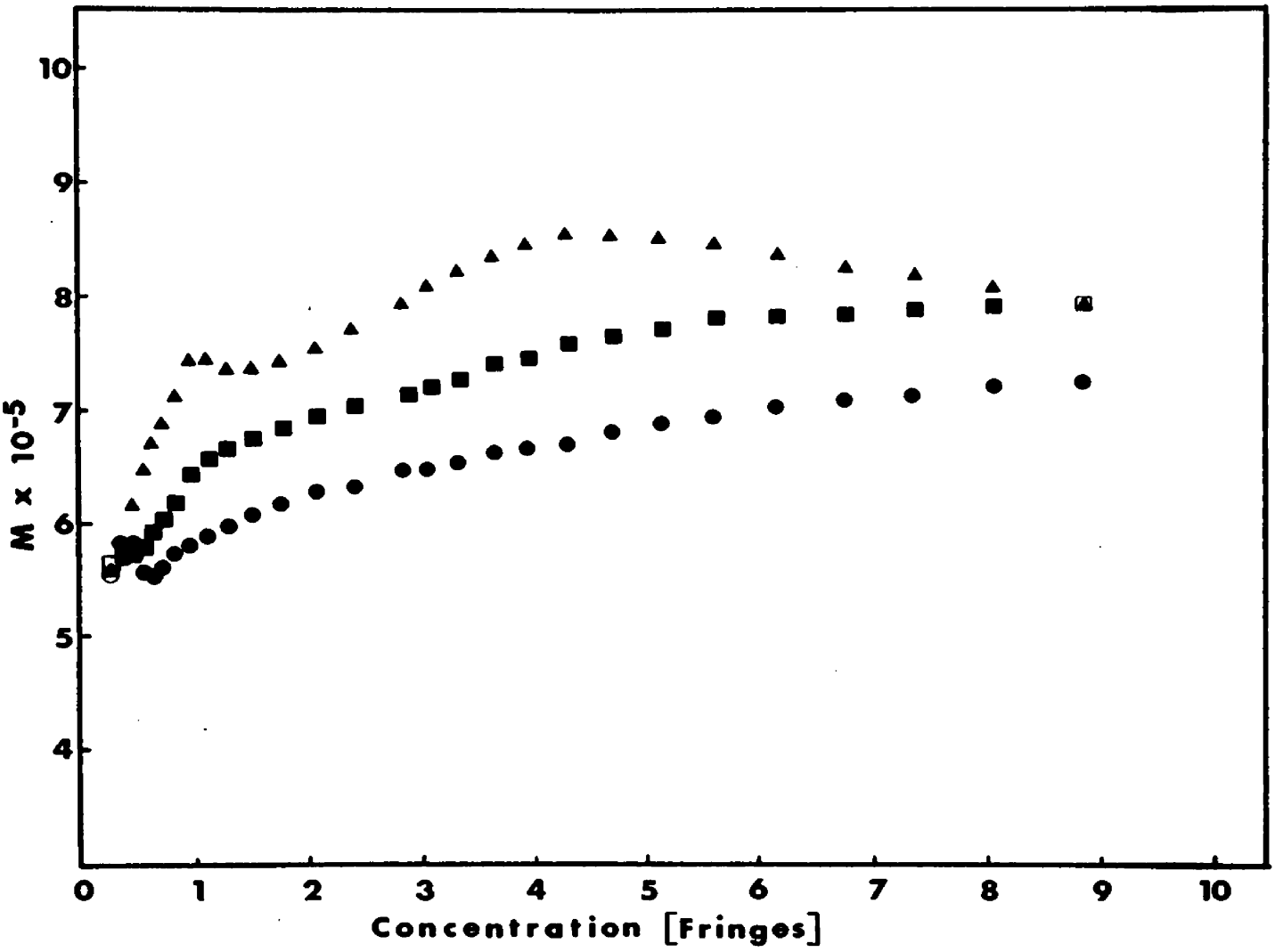

Figure 8. Number-, weight-, and Z-average molecular weights of the 23S particle as determined by sedimentation equilibrium; (●—●) number-, (■—■)weight-, and(▲—▲) Z-average molecular weights.

Both of these methods gave results similar to that found in Figure 8. Another 23S sample was run that was obtained from the zonal centrifugation of the sonicated particles. Because the sample was obtained from a sucrose gradient, it was believed that both protein and rRNA would be separated from the 23S particle. The effect of the sonication on these particles is not clearly known, however, the sedimentation equilibrium results showed the same heterogeneous solution.

There are two plausible explanations for the heterogeneity:

1. ribonuclease degradation of the samples results in more than one component
2. dissociation of the particle occurs during the equilibrium run.

There was no evidence for the former as schlieren patterns for the samples gave single, symmetrical peaks. If the latter explanation is correct, an alternative preparative method is needed to prevent such dissociation from occuring.

Because more than one component was present, it was necessary to analyze the data in a different manner. If only two species are present, the molecular weights of these two species can be determined, utilizing the point-average molecular weights across the solution column. This method is basically the two-species plot method developed

by Roark and Yphantis (107) and also utilized by Jeffry and Pont (53), and by Teller et al. (136).

It can be shown that if two ideal sedimenting species of molecular weights M_1 and M_2 with weight fractions of $[1 - \alpha(r)]$ and $\alpha(r)$, respectively, as a function of radial distance, r, that the number- and weight-average molecular weights can be written as follows:

$$\frac{1}{M_n(r)} = \frac{1 - \alpha(r)}{M_1} + \frac{\alpha(r)}{M_2}$$

$$M_w(r) = [1 - \alpha(r)] \; M_1 + \alpha(r) \; M_2.$$

Combining these two equations gives the relations:

$$M_w(r) = -M_1M_2 \; [1/M_n(r)] + M_1 + M_2.$$

Therefore, a plot of M_w versus $1/M_n$ for the points across the solution column gives a slope equal to $-M_1M_2$ and y-intercept equal to $M_1 + M_2$. The above equation can be written in the general case as:

$$M_k(r) = -M_1M_2 \; [1/M_{k-1}(r)] + M_1 + M_2,$$

where $M_k = M_n$, M_w, M_z, or M_{z+1} and M_{k-1} is the next lower average.

Another problem in this study is that of $\bar{v}$. The $\bar{v}$ for the 23S particle is 0.619. The two most probable

contaminating species are protein and/or rRNA that have partial specific volumes of approximately 0.73 and 0.57, respectively. Thus, a calculation of the molecular weight based upon the $\bar{v}$ of the 23S particle will give erroneous results. For this reason, the point-average molecular weights were determined with a value of $\bar{v}$ equal to 0, giving a value of the term of $(1 - \bar{v}\rho)$ equal to 1. These values will be referred to as point-average σ values. The values of σ were then substituted into the equations for the two-species plot. The weight-average molecular weights for the two species can then be found by using the appropriate value of $\bar{v}$, as:

$$M_{w_{1,2}} = \frac{\sigma_{1,2}}{(1 - \bar{v}\rho)_{1,2}}$$

The data of one equilibrium run were analyzed by the above procedure. Plots of σ_w <u>versus</u> $1/\sigma_n$ and σ_Z <u>versus</u> $1/\sigma_w$ were made as shown in Figure 9. The line drawn through these points in Figure 9 represents the best fit for all of the points.

The results of the two-species plots indicated that the two species had fairly large molecular weights. Therefore, the weight-average molecular weights were determined using values of $\bar{v}$ that correspond to the rRNA and the 23S particle. The molecular weights obtained by this procedure using the plot of σ_w <u>versus</u> $1/\sigma_n$ are 4.5×10^5 daltons and

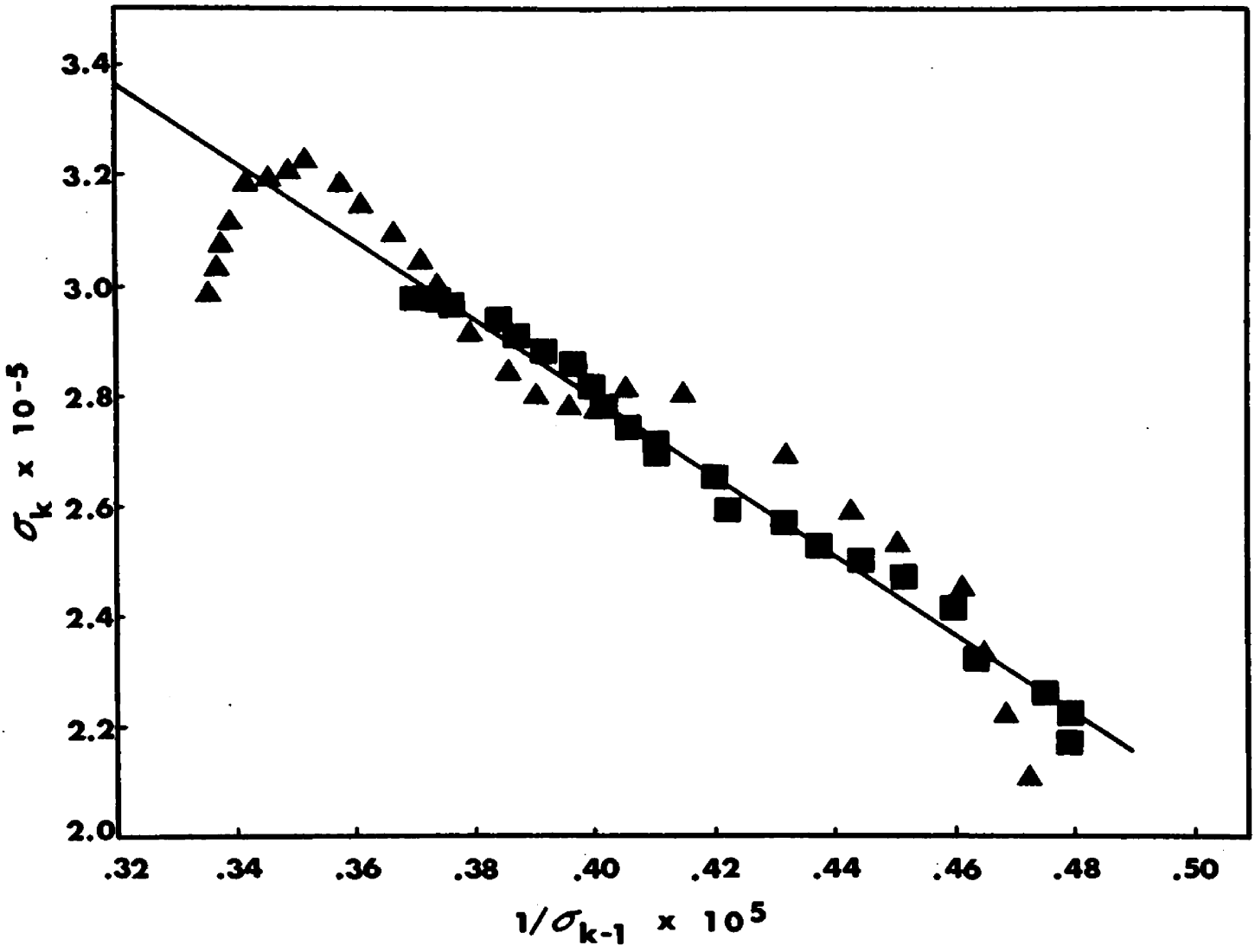

Figure 9. Two-species plot of the sedimentation equilibrium data: σ_w vs. $1/\sigma_n$ (■-■) and σ_z vs. $1/\sigma_w$ (▲—▲). The line represents a linear least-squares fit of the points.

9.7×10^5 daltons. The plot of σ_z *versus* $1/\sigma_w$ gives molecular weights of 4.6×10^5 and 10.4×10^5 daltons. Using both set of points molecular weights of 4.5×10^5 and 10.0×10^5 daltons are obtained.

It is not unreasonable to assume an error of ± 5% for the determination of the molecular weights by this two-species plot method. The molecular weight of the larger species would then correspond to the molecular weight of the 30S particle (45), within experimental error. The molecular weight for the smaller particle, however, does not agree, within experimental error, with the value of 6.4×10^5 daltons for 16S rRNA (98). This discrepancy could be due to the experimental conditions of the equilibrium run. The speed for the run was chosen for a particle having a molecular weight of 9×10^5 daltons. Assuming that the contaminant was rRNA, a higher speed would be necessary for an accurate determination of this species.

SIZE AND SHAPE OF THE 23S PARTICLE

The hydrodynamic properties of the 23S particle are related to the shape and hydration of the molecule. The values of the sedimentation coefficient, $s^\circ_{20,w}$, the intrinsic viscosity, [n], the partial specific volume, $\bar{v}$, and the molecular weight were used to estimate the shape and hydration of the 23S particle.

Small-angle x-ray scattering has been done on the unfolded 30S particle (120). Although this particle has been isolated in a different manner than the 23S particle of this study, it is believed that these two particles are similar, if not the same. These results are pertinent to this discussion of particular shape.

The anhydrous volume, as calculated from the molecular weight and $\bar{v}$, is 0.926×10^6 $\mathring{A}^3$. The volume of the uniform density parallelepiped as determined by Smith (120) is 3.46×10^6 $\mathring{A}^3$. A volume difference of this magnitude is due to hydration and asymmetry of the particle. However, there was reason to believe that some error in the shape and volume of this 16S particle was present due to the assumption of a uniform-density particle. Therefore, it is of interest to discuss the shape of the 23S particle as calculated from the hydrodynamic values.

From the molecular weight and the sedimentation coefficient, the frictional ratio, f/fo, of the particle can be determined by the following relationship (132):

$$f/fo = 1.19 \times 10^{15} \left(\frac{M^{2/3} (1 - \bar{v} \rho)}{s^{\circ}_{20,w} (\bar{v})^{1/3}} \right) \qquad (1)$$

The frictional ratio is separated into two parts which can be formulated as follows:

$$f/fo = \left(\frac{f}{fo} \right)_s \cdot \left(\frac{f}{fo} \right)_h \qquad (2)$$

where s and h signify the frictional ratios for the shape and hydration factors, respectively. The frictional ratio due to hydration is given by the relationship:

$$\left(\frac{f}{fo}\right)_h = \left(1 + \frac{\delta}{\bar{v}\rho}\right)^{1/3} \qquad (3)$$

where δ is the hydration as grams of water per gram of ribonucleoprotein. Because the effect of shape has been formulated by Perrin (104) for ellipsoids of revolution, this discussion will be limited to those mathematical models.

The intrinsic viscosity also contains information about the size and shape of the hydrodynamic particle. The effect of asymmetry and hydration on intrinsic viscosity can be expressed by the equation:

$$[\eta] = \sigma(\nu) \quad (\bar{v} + \delta\bar{v}_o) \qquad (4)$$

where $\sigma(\nu)$ is the Simha factor and $\bar{v}_o$, the specific volume of the solvent. This and the previous equation can be re-written to give values for the water of hydration as follows:

$$\delta = \left(\frac{[\eta]}{\sigma(\nu)} - \bar{v}\right) / \bar{v}_o \qquad (5)$$

and

$$\delta = \bar{v}\rho \quad [\ (f/fo)_h^3 - 1] \qquad (6)$$

The effective particle volume can also be calculated from the hydrodynamic parameters. A hydrodynamic volume can be obtained using the sedimentation coefficient and the molecular weight from the relationship:

$$V_s = \left(\frac{M\ (1-\bar{v}\rho)}{Ns} \right)^3 \ / \ 162\ \pi^2\ P^3(\nu) \qquad (7)$$

where $P(\nu)$ is the Perrin function. The particle volume, utilizing the intrinsic viscosity, is:

$$V_\eta = \frac{M\ [\eta]}{N\sigma(\nu)} \qquad (8)$$

where $\sigma(\nu)$ is the Simha factor. A third relationship utilizing the partial specific volume gives:

$$V_h = \frac{M}{N}\ (\bar{v} + \delta\bar{v}_o) \qquad (9)$$

where $\bar{v}_o$ is the specific volume of the solvent.

From the above equations one can calculate the axial ratio and/or the water of hydration for the 23S particle. Because a parallelepiped does not easily fit into the configuration of an ellipsoidal model, we were not justified in using the dimensions determined by Smith (120). To determine axial ratios, one must estimate the hydration value. An estimate of both parameters, however, can be made utilizing the method of Mehl, Oncley, and Simha (81), where the hydration of rigid ellipsoids of evolution, determined from viscosity and sedimentation, are plotted

versus axial ratio. The overlapping areas of pairs of such curves include the possible choices for shape and hydration.

The hydration values, as determined from the intrinsic viscosity, are determined directly from equation (5) utilizing the tabulated values of $\sigma(\nu)$ (81). The hydration values, as determined by sedimentation, were calculated utilizing equation (6), after the values of $(f/fo)_h$ were determined from equations (1) and (2). The fractional ratio, f/fo, was calculated to be 2.03 using a value of $M=8.5 \times 10^5$. This value was chosen because of the uncertaintly of our molecular weight determination. The values of $(f/fo)_s$ are those calculated from Perrin's equation (104) and tabulated by Svedberg and Pedersen (132).

A plot of the axial ratios versus hydration is shown in Figure 10. Relative experimental errors of ± 7% were included in the values of hydration as determined in the hydration values determined from sedimentation, and errors of ± 5% were included in the hydration values determined from viscosity.

The fact that the curves do not cross indicates that our errors are larger than calculated, or that the ellipsoidal models are not representative of the 23S particle. If we assume the value of the water of hydration to be 1.4 g H_2O /g RNP, the same value as determined for the 30S subunit (120), we can determine the shape for the 23S particle from

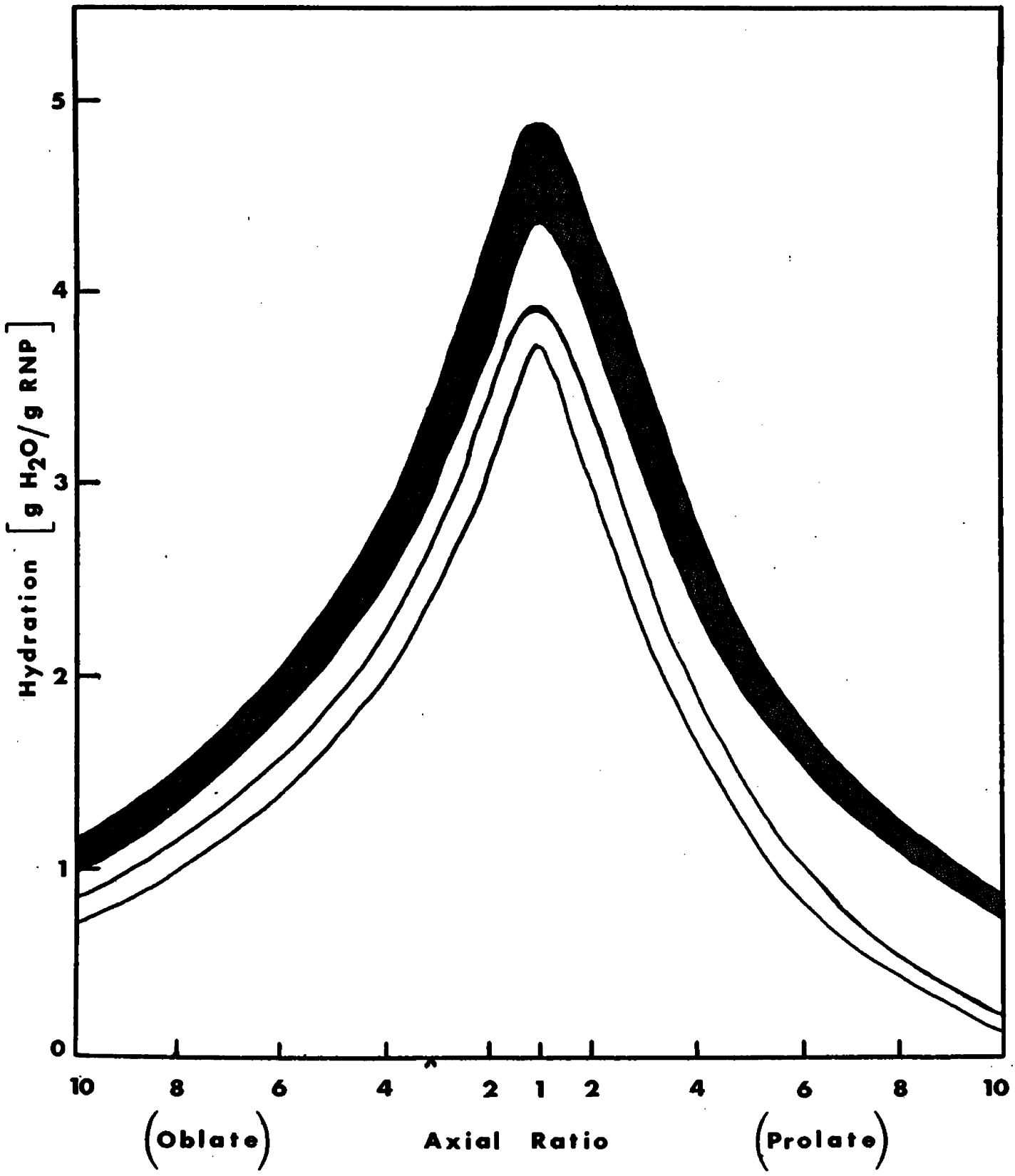

Figure 10. A graph of hydration versus axial ratio for the 23S particle: the shaded area was determined from viscosity (ν), and the white area was determined from sedimentation (f/f_o).

the graph of Figure 10. We find the oblate ellipsoids with axial ratios of 8:1 and 6:1 and prolate ellipsoids of 7:1 and 5:1 fit the data for this value of δ. The average axial ratio agrees fairly well with that determined by Smith (120).

The hydrated volumes of these ellipsoids are 3×10^6 $\mathring{A}^3$ as calculated from equations (7) and (8). The hydrated particle volume as calculated from equation (9) is also 3×10^6 $\mathring{A}^3$ (120). The volumes calculated from the 23S particle obtained in low Mg^{++} (this study) and the volume of the unfolded particle obtained with EDTA (Smith, 120) appear to be in the same range. However, this agreement is quite possibly totally misleading. The volume of the uniform density parallelepiped, representing the particle in solution as seen by x-rays, corresponds to the volume in which there is an average electron density greater than the surrounding medium. This volume includes the ribosomal particle and volume occupied by the solvent within the subunit. Our calculated hydrodynamic volumes include both the internal and external hydration. Therefore, if these particles are similar, it would appear that no external hydration exists. This seems improbable as the 30S subunit has approximately 60% external hydration. It is more likely that the volume calculated from small-angle x-ray scattering is much to high, due to the assumed shape or the radius of gyration. On the other hand, the two particles may be totally dissimilar, and our comparisons are not justified.

In either case, further analysis seems necessary to explain the volume discrepancies of the unfolded particles.

SONICATED 23S PARTICLES

Sonication of the 23S Particle

The results of the sonication, as shown in Figure 3, gave two major particles other than the fastest sedimenting 23S particle. A slower sedimenting particle is also present in the schlieren pattern. The sonication was tried for various periods of time at different intensity settings, but it was found that the maximum setting gave the best results. The duration of sonication was important and varied slightly with the sample. Each sample was monitored via sedimentation velocity experiments to determine if the sonication time was sufficient to produce slower sedimenting particles. It was found that increased periods of sonication gave proportionately decreased amounts of 23S particles and increased amounts of slower sedimenting particles. However, the time of sonication was limiting in the sense that further breakdown of all the particles occurred with total degration observed with extreme conditions. Therefore, 20 to 25 minutes of sonication was deemed sufficient and optimal.

The 30S particle was subjected to sonication with similar conditions as used for the 23S particle in order to

determine if sonication was loosening or disrupting the particle. No significant difference was seen in the schlieren patterns of the 30S particle before and after sonication.

The separation of the sonicated 23S particles with zonal centrifugation as described previously gave good separation as shown in Figure 11. The schlieren patterns of the isolated particles are shown in Figure 3. The uncorrected sedimentation coefficients of these particles are 4.5, 9.4, 15, and 23S. These particles will be referred to as the 5S, 10S, 15S, and 23S particles, respectively.

RNA and Protein Concentration Determinations

The RNA and protein determinations were found as described in Chapter III. The values of 33% protein and 67% RNA (63) for the 30S particle give a ratio of protein/RNA of 0.49. The values determined for the 23S particle and sonicated particles are given as the ratio of protein/RNA in Table 1. The value of 0.50 for the 23S particle was obtained using an $E^{1\%}_{260}$ = 145 for the particle giving 33% protein and 65% RNA. The value for the RNA is slightly low, but is within experimental error. Because the extinction coefficients for the 5S, 10S, and 15S particles were not determined, there was no way to determine the actual percentages of protein and RNA. However, the ratio for the 10 and 15S particles are close to that for the 30S, indicating

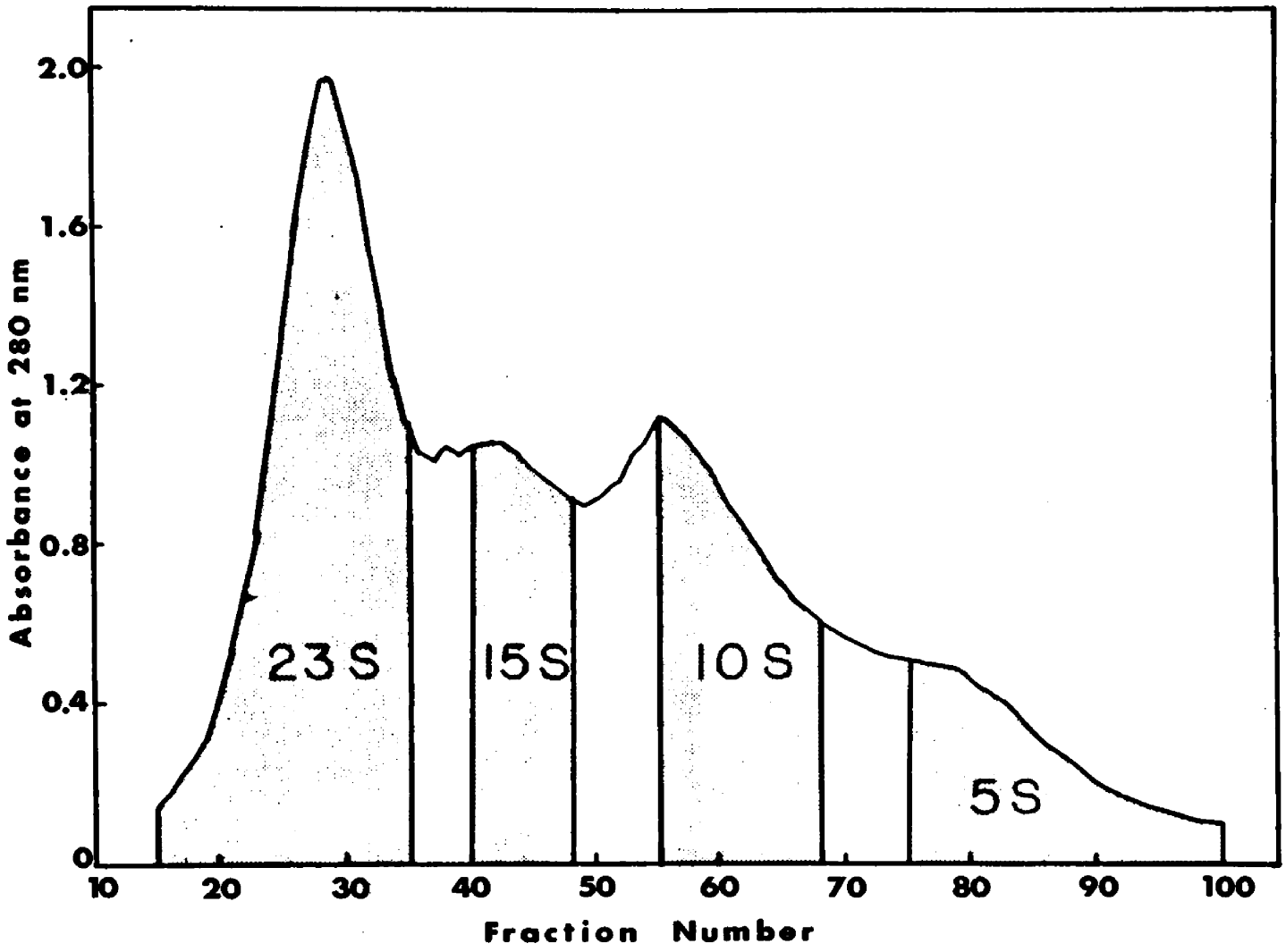

Figure 11. Sucrose gradient elution profile from zonal centrifugation of particles derived from the sonication of the 23S particle. The separation of the particles was done on a 10-30% sucrose gradient in a Ti-15 rotor. The shaded areas represent those fractions used for further study.

the relative amounts of protein and RNA are the same. On the other hand, the 5S particle shows a much lower ratio of protein to RNA.

Table 1. Determination of protein and RNA concentrations by methods of Lowry (74) and Mejbaum (82).

Particle	% Protein	%RNA	µg. Protein/µg. RNA
30S[a]	33	67	.49
23S	33	65	.50
15S	--	--	.47
10S	--	--	.47
5S	--	--	.16

[a]The values for the 30S particle are those determined by Kurland (63).

Acrylamide Gel Electrophoresis

Gel patterns for the 30S proteins, the 23S proteins, and the sonicated particle proteins are shown in Figure 12. Protein identifications were made on the basis of the comparisons described by Wittman et al. (151) and the gel patterns shown by Voynow and Kurland (146) and Schendel et al. (114). The gel patterns for the 30S proteins are not exactly the same as we obtained. However, our assignment was made by comparing our gels of the 30S proteins with the published results. The protein identification of the other particles was then made by comparisons to the electrophoretic

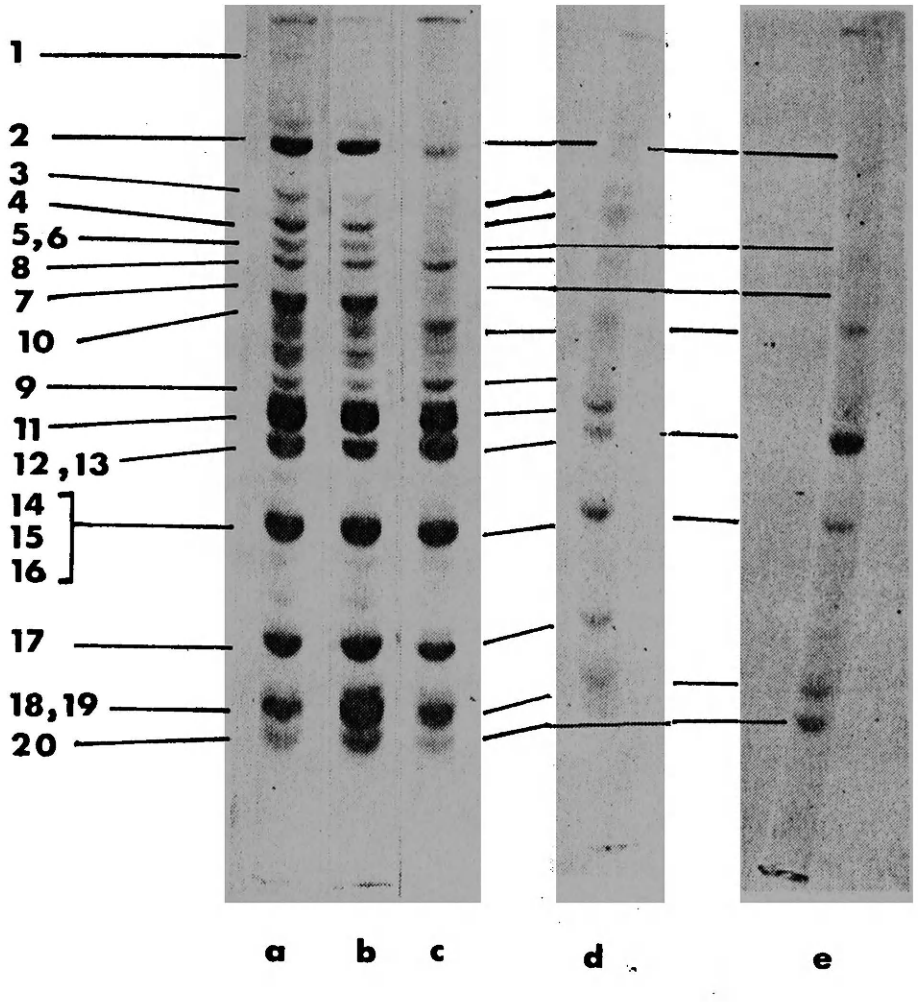

Figure 12. Acrylamide gel electrophoresis of proteins from the 30S subunit, 23S unfolded particle, and the sonicated 23S particles: a) 30S proteins b) 23S proteins c) sonicated 23S proteins d) 15S proteins e) 10S proteins.

pattern obtained for the 30S proteins. Although our method of assignment of protein bands might be slightly ambiguous, the identification of the proteins are consistent with our 30S subunits. The results at this time are tentative. However, we do feel the identifications of the proteins are fairly good.

It was found that the preparative procedure altered the gel patterns of the 30S proteins. The difference can be seen in Figure 12a and 12b. The proteins in Figure 12a are from 30S subunits that underwent 8 hours of washing in 0.5 M NH_4Cl, while those in Figure 12b are from 30S subunits that were washed for 12 hours in 0.5 M NH_4Cl. The main difference between the two seems to be a loss of 3 to 5 bands near the top of the gel pattern of the 12 hour washed subunits. This confirms Kurland's findings (63) that high salt wash does indeed remove proteins.

The basis of our identifications were made from the patterns obtained with the "hard", 1.5% bis-acrylamide gels. The "soft", 0.75% gels, were not used since ambiguous results were obtained when we tried to identify the proteins of the sonicated particles by comparison to the gel patterns of the 30S particle. The electrophoretic pattern of the "hard" gels gives 15-16 bands as certain proteins migrate at the same rate. The relative intensity of a band is indicative of the amount of protein present and can be used for subjective identification of a protein. Densitometric tracings

of the stained gels to quantitate the differences between protein bands were not done, but visual interpretation of the relative intensities was used in the determination of the proteins.

From the gel patterns of Figure 12, it can be seen that proteins S3, S4, and S8 are not present in the 10S particle. The band for proteins S5 and S6 and the protein band for S7 are absent in the 15S gel but are faintly present in the 10S gel. Because S5 and S6 are not differentiated, both proteins are assigned to the 10S particle. It is ambiguous as to whether both proteins S9 and S11 are resolved, but this band is relatively more intense in the 15S particle than in the 10S particle, and these proteins are assigned to the 15S particle. The band for proteins S12 and S13 are present in both gels but of greater relative intensity in the 10S particle. This could possibly suggest only one of the two proteins are associated with the 15S particle, however, these proteins are assigned to the common group. The band for proteins S14, S15, S16, and S17 is similar to the S12, S13 band, but the intensity is much lighter for the 10S particle. Protein S17 has a greater relative intensity in the 15S gel, whereas, S20 is present to a greater degree in the 10S particle. A summary of the proteins found in each of the particles studied is shown in Table 2.

Table 2. Proteins found on the particles isolated from the sonication of the 23S particle. The unique proteins are those found only on one particle and not the other. The common proteins are those found on both particles.

15S Particle Unique Proteins	Common Proteins	10S Particle Unique Proteins
S3	S2	S5
S4	S10	S6
S8	S12	S7
S9	S13	S20
S11	S14	
S17	S15	
	S16	
	S18	
	S19	

CHAPTER V

DISCUSSION

Physical Characterization of the Unfolded Particle

The results of this study demonstrate that the 30S subunit undergoes an extensive conformational change upon exposure to low Mg^{++} concentrations. It is believed that this conformational change is representative of a loosening or unfolding of the tertiary structure of the ribosome. Although unfolded particles have been previously observed in various buffer systems, a thorough study to determine the properties of these particles has not been done. In this study, a number of physical properties to characterize the unfolded particle have been determined.

The sedimentation coefficient ($s^{\circ}_{20,w}$) decreases from 31.8S (45) to 23.3S while the intrinsic viscosity increases from 8.1 (45) to 11.0 ml/g. Both observations are consistent with the idea of a loosened conformation of the ribosomal subunit. The large change that occurs in these physical parameters indicates that the 23S particle is more asymmetric and/or hydrated than the 30S subunit. Based on the assumption that the hydration is unchanged from the 30S subunit, the 23S particle has a calculated axial ratio of approximately 7:1. The axial ratio is close to that determined with small-angle x-ray scattering (120) of the unfolded particle obtained from exposure of the 30S subunit to EDTA.

The axial ratio for the 23S particle was calculated using the assumption that the unfolded particle could be approximated by a simple ellipsoidal model. Conversely, the unfolded particle obtained from EDTA exposure approximated a parallelepiped having sides in the ratio 1:4:8 (120). A 23S "core" particle, which was obtained by removing 30-40% of the protein from the 30S subunit, was also found to be more extended than the 30S subunit and was approximated by a 1:4:8 triaxial ellipsoid (120). The parallelepiped or the triaxial ellipsoid may be suitable models for the 23S particle in this study. Whatever the case, it would be impossible to calculate an exact axial ratio from our data. This significant factor, however, is that the 23S particle exhibits greater asymmetry than the 30S subunit with an increase of at least 50% in the axial ratio.

The measured value of 0.619 ml/g for the partial specific volume of the 23S particle is significantly higher than the value of 0.591 ml/g measured for 30S subunit (45). This would indicate that the density of the unfolded particle is less than that of the intact subunit. The hydrodynamic volume calculated for the 23S particle is approximately 2400 ml/mole of 23S greater than that of the 30S subunit, as calculated from the intrinsic viscosity (120). This increase in volume would represent an increase of approximately 0.03 ml/g, which is the measured difference of the $\bar{v}$ between the 23S and 30S particles. The calculated

volumes for these particles contain a certain amount of error and, thus, the change in the particle volume should not be regarded as solely responsible for the density difference between the intact subunit and the unfolded particle. Any disruption of protein-protein and/or protein-rRNA interactions during the unfolding process could also account for the density decrease.

The value of the extinction coefficient is the same as measured for the 30S subunit (45). This is consistent with the idea that the unfolding process affects the tertiary structure of the subunit but does not disrupt the secondary structure of the rRNA.

The molecular weight determined by sedimentation equilibrium, utilizing the two-species plot of M_w versus $1/M_n$, gives a value of 9.7×10^5 daltons for the 23S particle. This value appears to be within experimental error of the molecular weight for the 30S particle (45). Although the molecular weight for the 23S particle is higher than the value for the 30S subunit, the exact experimental error is not known. Thus, the molecular weight of the unfolded particle could be less than the subunit due to a loss of RNA and/or protein. However, a probable minimum for the molecular weight seems to be 8.3×10^5.

If a large piece of RNA with a molecular weight of approximately 70,000 was sheared from the particle during the preparative procedure, the evidence of such a fragment

should be seen in the sedimentation velocity experiments. However, no such particle was observed. Although ribonuclease digestion could cause a decrease in the molecular weight, the 23S particles were quite stable indicating the lake of such enzymatic activity.

The loss of proteins(s) from the subunit during the unfolding process is a more probable factor that could cause a decrease in the molecular weight. If the factors involved in the binding of the protein are considered to be protein-RNA or protein-protein interactions, it is possible that a partial disruption of such intimate forces occurs when the 30S subunit is structurally altered, allowing some proteins to diffuse away. The studies of Nomura and coworkers (96, 140) have indicated a protein-ribosome structure interdependence that might allow such protein loss in unfolding the 30S subunit.

The acrylamide gel electrophoresis showed no quantitative difference between the proteins of the subunit and the 23S particle. Differences in the relative intensities of protein bands between the 30S and 23S particles were observed and might be considered as indicative of a protein loss. Protein S1 and possibly S21, however, were found to be absent from the 23S particle. Because S1 and S21 are fractional proteins, one can not assume that a loss of these proteins will decrease the molecular weight of the particle by an amount equal to the mass of the two proteins.

The weight-average molecular weights of S1 and S21 are 65,000 and 20,000 daltons, respectively, and are present in the ribosomes at approximately 0.1 copy per ribosome. Thus, the molecular weight of the 23S particle could not be expected to have a molecular weight that is less than 8.9×10^5 daltons due to the loss of these two proteins. This same argument can also be applied to the fractional proteins as a whole. If all fractional proteins were lost during the unfolding process, one would expect a net decrease of approximately 70,000 daltons.

The scheme of unfolding presents an interesting picture. It seems appropriate to think that an RNP strand on the periferal portion of the ribosome unfolds and extends away from the main portion of the ribosome. Because the small dimension of the 30S subunit and the EDTA-unfolded subunit have been shown to be essentially the same by small-angle x-ray scattering (120), we may assume that the 23S particle of this study is similar. The 50 Å small dimension of these particles corresponds approximately to a monoprotein layer that is held together by rRNA. As Kurland has pointed out (65), the average ribosomal protein has a molecular weight of 20,000 with an average $\bar{v}$ of 0.74 ml/g, which would correspond to an anhydrous globular protein with a diameter of 36 Å. Addition of the hydration factor would effectively increase the diameter of the protein. Because the protein accounts for a large part of the small dimension, it is feasible that the unfolded portion of protein and rRNA also has a small

dimension of 50 Å. The 30S subunit has been approximated by a 1:4:4 oblate ellipsoid and appears to be essentially planar. Although the unfolding process appears to occur in one dimension, we can not assume that the loosened portion of RNP lies within the same plane as the main body of the ribosome. Thus, it is easy to picture the unfolded subunit as a very thick, bent coin.

Sonicated Particles

The schlieren pattern of the sonicated 23S particle shows four peaks with the fastest sedimenting peak being the 23S particle. This pattern indicates three possibilities as to the nature of sonication on the 23S particles.

The first possibility is that of further unfolding of the 23S particle. The 15S particle sediments at a rate similar to the 16S particle that has undergone further change, possibly in the secondary structure of the RNA. The 5S particle seems to be too small to say that further structural change occurs in the RNP particle. However, the 5S particle could be the result of total degradation of any of the other particles.

Another possibility is that the 23S particle undergoes further unfolding to the 16S stage followed by strand cleavage resulting in the 10S and 5S particles. One would expect the ratio of these particles to be one to one if this were the case. The relative peak areas are clearly not of this proportion, although this is not entirely indicative

of their absolute number ratio, as the ratio of the peak area to the weight of the particle is a true measure of the concentration.

The third possibility is that the 23S particle undergoes cleavage producing two or three different fragments. The 5S particle was found to have some protein present, although we were unable to determine any protein by acrylamide gel electrophoresis. It might be thought of as a product of degradation, or secondary cleavage of one of the other particles, or a primary product of cleavage. If it is assumed that sonication gives two primary fragments and that the 5S particle is due to some type of degradation, the relative peak areas in the schlieren pattern is disturbing in that the 10S peak area is much greater than the 15S peak area. If only the two particles are the product of sonication, one would expect a ratio of one to one. A possible explanation for this discrepancy could be due to an anomaly of the ultracentrifuge, the Johnston-Ogston effect. However, the combined peak areas of the 15S pattern and the 5S pattern are approximately equal to the area of the 10S pattern which could indicate that sonication does result in three unique particles.

At this point we are unable to clearly define the process of sonication on the 23S particle. The fact that the 10S and 15S particles have unique complementary proteins

associated with them indicates that these molecules are fragments of the 23S particle. The inability to find the proteins on the 5S particle indicates that further work is needed in this direction to determine the origin of this molecule. Molecular weight determinations of these sonicated particles would clearly help to define the plausibility of whether or not these particles are fragments. Because of the difference in proteins, however, we tentatively believe that the 10S and 15S particles are unique fragments.

The 10S and 15S fragments have unique proteins but also have proteins that are common to both. If these fragments are different, an explanation is needed as to why sonication does not produce two fragments with totally unique, complementary proteins. A feasible explanation for this fact is that sonication breaks the RNA strand at more than one site, but that each 23S particle undergoes only one cleavage per molecule. Thus, depending on the site of cleavage, certain proteins may be associated with either fragment. Table 2 shows 9 proteins thought to be common to both particles. This would indicate two possibilities for cleavage; a large number of cleavage points or two different cleavage points separated by a long RNP strand.

If the 23S particle is thought to have an extended loop of RNP strand, a most likely place for cleavage would be along that extended loop. A schematic representation of the cleavage points is given in Figure 13. The first

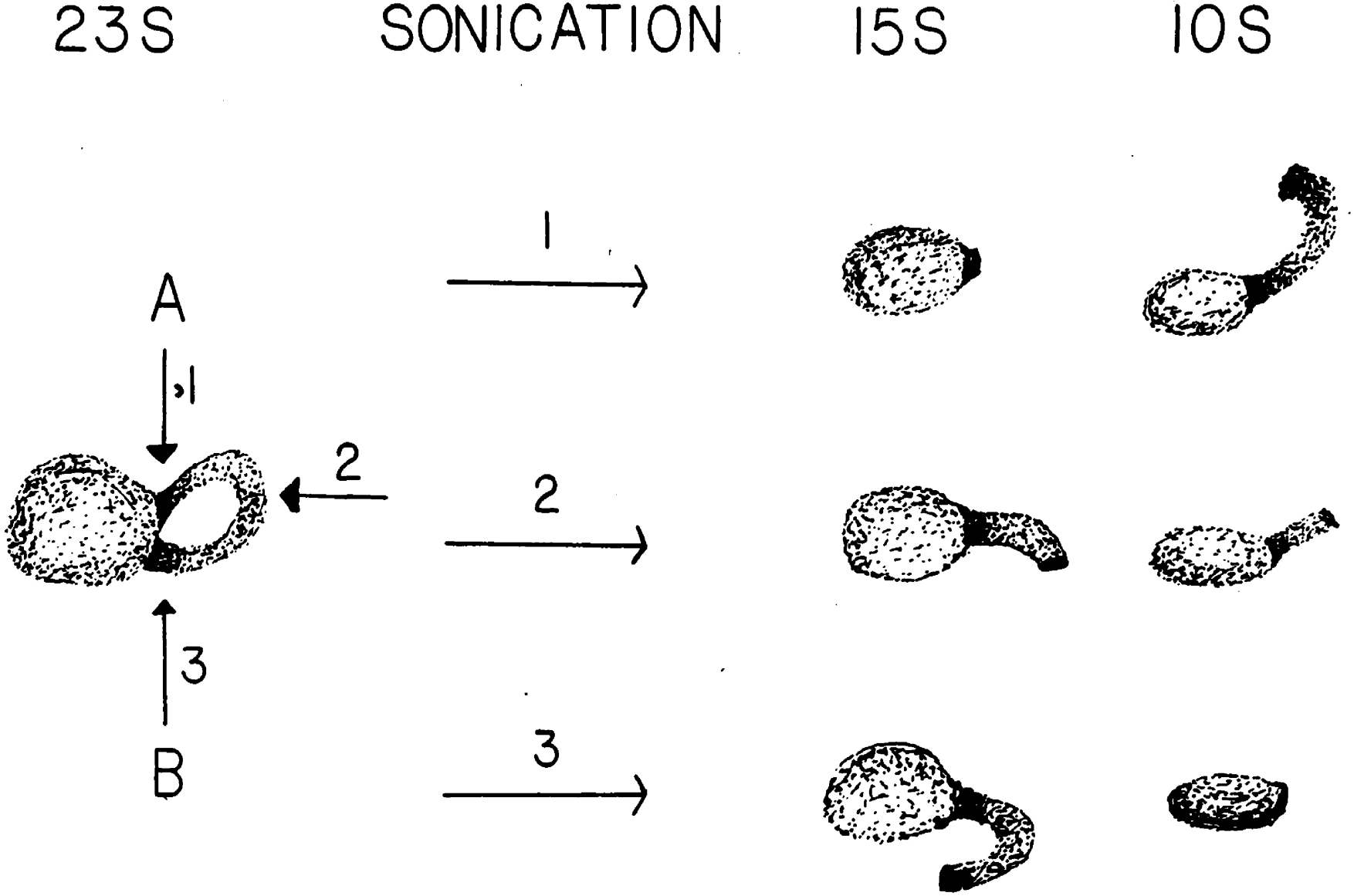

Figure 13. Schematic representation of the sonication of the 23S particle. For an explanation, refer to the text.

possibility is shown by cleavage occurring at all the arrows, resulting in particles with various lengths of the broken strand. A piece of strand that can encompass 9 proteins would have to be fairly large, resulting in particles of various molecular weights. The second possibility is that cleavage occurs only at points A and B. This type of cleavage would result in a particle that would vary in its molecular weight by the molecular weight of the strand between the cleavage points. Our results indicate that these particles are fairly homogeneous which dictates gross structural change in a particle to give the same sedimentation coefficient.

Although these two possibilities are feasible if not correct, another explanation for the sonication results can be found. The acrylamide gel electrophoresis does not separate some of the proteins common to both fragments. The intensity of some of these bands is possibly indicative of proteins present or absent in the fragments. It seems worthwhile to postulate as to which fragment certain of the common proteins could be associated. Table 3 lists the assigned proteins to their respective fragments. This assignment illustrates the fact that possibly the large number of common proteins is due to our inability at this time to identify some proteins. If this is the case, sonication could be introducing a nick at only one point along the RNP strand.

Table 3. A postulated assignment of the common proteins found in both of the sonicated particles. The proteins assigned to each of the particles are those proteins that migrate at the same rate and can not be distinguished.

10S Particle Unique	Common	15S Particle Unique
S12	S2	S13
S14	S10	S15
S19		S16
		S18

If only one nick occurs in the RNP strand with sonication, the requirement to unfold a loop of RNP for the 23S particle is diminished. If a strand continuous with either the 3' or 5' end of the rRNA is unfolded and sheared, the same results could be obtained. The major drawback to this hypothesis is the size of strand that would have to be unfolded that could accommodate the proteins found to be associated with the 10S fragment, assuming the 10S arises from the extended strand. On the other hand, the 5S particle would be a good possibility for the fragment produced from an end-terminal cleavage. This type of breakage should result in only two particles, however, and not three as observed. Therefore, at this time, the best model to fit both the physical studies and the sonicated particle protein

studies is that of a particle with an extended loop of RNP. From our data, we must also assume that more than one break occurs in the strand, resulting in two fragments with proteins common to both. It is evident that more acrylamide gel studies, especially two-dimensional electrophoresis, are needed to resolve the ambiguous proteins to help determine if these fragments are the results of one or more breaks in the RNP strand.

During the course of this work, various workers have published papers on RNP fragments derived from the 30S particle by ribonuclease treatment. It is worthwhile to discuss the results of these studies in comparison with our data.

Zimmermann, Muto, Fellner, Ehresmann, and Brenlant (153) have determined binding sites on the 16S ribosomal RNA for six proteins by limited ribonuclease hydrolysis of RNA-protein complexes, as well as by the interaction of individual proteins with RNA fragments purified from partial enzymatic digests. They found that proteins S4, S8, S15, S20, and, probably, S13 bind within a fragment that comprises some 900 nucleotides and covers almost the entire 5'-terminal portion of the 16S molecule. An RNA fragment derived from the 3'-terminal portion of the 16S molecule was believed to be the binding site for protein S7. Protein S7 was found to co-sediment primarily with the 3-'terminal fragment when

complexes of RNA and protein were digested, but would not bind with the same piece of RNA prepared from uncomplexed RNA. Our results show proteins S4 and S8 associated with the 15S particle, and protein S7 associated with the 10S particle. Proteins S13 and S15 were not differentiated in our gels but were classified as being common to both particles. Using the study of Zimmermann et al. as a guide, one can postulate that the 15S particle is that portion associated with the 5'-terminal end and the 10S particle, the 3'-terminal. Because protein S20 was found to be present on the 10S fragment and only faintly present on the 15S fragment, protein S20 was assigned to the 10S particle. The discrepancy of relative binding position relative to the terminal end of the RNA can be thought of as the results of different cleavage points along the RNA strand. If the cleavage point incurred with sonication is to the 5'-terminal end of the binding site, S20 would then be associated with the 3'-terminal particle.

If proteins S13 and S15 are common to both the 10S and 15S fragments, an interpretation would have to be that the sonication can cleave the RNA strand at points 3' to S15 or 5' to S13. Although the position of binding for protein S7 is questionable, an interpretation of our results based on those of Zimmerman et al. is plausible. Although the proteins studied by this group have highly

specific binding sites and are those proteins which are bound first in the reconstitution of the 30S ribosome, the position of these binding sites may be somewhat in error. Only a little more than half of the nucleotide sequence of the 16S RNA is known, and, therefore, certain errors in the nucleotide sequence would alter the relative binding sites for the proteins. The 5'-terminal half of the RNA sequence is supposedly well understood, and, therefore, the binding sites of those proteins are most likely accurate.

Schendel et al. (114) have obtained three RNP fragments from the 30S ribosome by ribonuclease digestion. It was found that these three particles had overlapping regions containing the same proteins. They felt that each of the three particles were linear RNP strands, and with the overlap were able to postualte a protein sequence for the 30S ribosome. They have stated that to obtain an accurate linear map of proteins that many more overlapping fragments are needed. In comparing our results with theirs, agreement is not very good. A slight rearrangement of their map, however, will allow proteins S5, S6, S7, and S20 to be in the same region of the map which agrees with our findings of the proteins on the 10S particle. This rearrangement will also allow proteins S3, S8, and S9 to be in the same region which is consistent with our 15S particle. A major inconsistency is protein S4, which is located in the middle

of their map. No rearrangement can bring about an agreement between our results and theirs. Protein S11 is also in disagreement, however, our assignment of protein S11 to the 15S particle was made on the basis that both proteins S9 and S11 migrate at the same rate. However, Schendel et al. stated that their assignment of protein S9 and S11 was subjective, based on the fact that S11, in pure form, migrates more slowly than S9. Also, the staining of S9 is much more intense than that of S11. It is possible that the faint band in our gel for S9, S11 in the 10S particle is due to protein S11 and that S11 should be assigned to the 10S particle. Schendel and coworkers have also reported a manuscript in preparation by C.T. Shih and G.R. Cravan that proteins S21, S18, and S11 are sufficiently close neighbors to form a single group and undergo intermolecular cross-linking induced by reagent tetranitromethane. They have placed this group of proteins at the 3' end which would agree with our results if S11 is assigned to the 10S particle.

Postulating a linear sequence as done by Schendel et al. can lead to possible errors due to the heterogeneity of the ribosomal proteins. The fractional proteins are present in less than 0.6 copies per subunit indicating that the 30S subunit does not in fact contain 21 proteins, and the lack of sufficient protein present on an RNP strand

may lead to errors in the interpretation as to the presence or absence of a specific protein. This possible error can affect the linear sequence greatly as overlapping protein regions are used to determine the sequence. There is also the possibility that some proteins do not have a specific region on the RNA strand, resulting in errors in a sequence map. Overall, it appears premature at this time to consider the protein sequence map of Schendel et al. as correct.

Morgan and Brimacombe (91) have also treated 30S subunits with ribonuclease, resulting in nine RNP fragments. They have taken their data and applied it to the "assembly map" of Nashimota, Held, Kaltschmidt, and Nomura (93) with hopes of generating a partial topography of the 30S ribosome. A discussion of the fragments obtained is pertinent to this study.

On two fragments they have found proteins S5 and S6 on one and S6 and S20 on the other. This is in direct agreement with those proteins found on our 10S particle. On their particle number five, they have found proteins S7, S9, S20, and two of the three proteins S13, S14, or S19. On particle number nine, they found proteins S6, S8, S20, S15, and S16 or S17. Major discrepancies between our and their results is that of protein S9 in particle number 5 and protein S8 found in particle nine. Both of these proteins were found in our 15S particle. Four of their other particles showed agreement with both proteins S7 and S9.

There are three possibilities as to why the results are in direct disagreement. The most obvious possibility is that one of us is wrong in the assignment of protein S9. Another probable event is that the cleavage points of the RNA strand is sufficiently different so as to allow protein S9 to be associated with protein S7. A similar arguement can be used for the association of S8 with S20 and S6. Bickle, Hershey, and Traut (4) have concluded from protein cross-linking experiments that proteins S6, S7, and S9 are adjacent in the ribosome, and that S9 is adjacent to S5. Similarly, Lutter, Zeichhardt, Kurland, and Stoffler (76) have shown that proteins S5 and S8 are also closely related. If one thinks of the crosslinking experiments to occur among proteins that are associated on the same relatively short stand of RNA, these results are in disagreement with our findings. However, there is a third possibility that can explain the discrepancies among the results of Morgan and Brimacombe (91), the crosslinking experiments, and the results we have obtained. For simplicity, assume that the proteins found on the 15S particle are associated with the 5' end of the RNA strand and that the proteins on the 10S particle are associated with the 3' end, with a sufficient length of rRNA between the two to allow the 5' and 3' ends to be associated. Ribonuclease digestion could result in a single particle that contains two separate strands of RNA, the 5' end and the 3' end of the 16S rRNA. This could

account for the fact of why Morgan and Brimacombe (91) find protein S9 and S8 associated with the proteins found on our 10S fragment. The crosslinking experiments could also indicate such an assumed structure, in that proteins S6, S7, and S9 would be adjacent due to the folding of the RNP strand. A similar argument could pertain to the cross-linking between proteins S5 and S8.

Such arguments are entirely speculative. However, they are not in disagreement with the "assembly map" of Nashimoto et al. (93). Proteins S8 and S7 bind to the 16S rRNA directly and make major contributions in the binding of proteins S5 and S9, respectively. Our data suggests that major folding of the RNA is a requirement for this binding. It is evident that the studies of RNP fragments combined with crosslinking data can give useful information on the relationship of not only the proteins but of relative areas of the rRNA. Sufficient data of this type combined with the physical studies of unfolded particles and particle fragments should hopefully give enough information to give a three dimensional structure of the 30S ribosome.

CHAPTER VI

SUMMARY

The 30S ribosomal subunit of Escherichia coli undergoes an extensive conformational change upon exposure to low Mg^{++} concentration. Dialysis of the subunit against a buffer containing 0.0001 M $MgCl_2$, 0.07 M KCl, 0.01 M Tris-HCl, pH 7.4, resulted in an unfolded particle that was characterized by determining a number of its physical parameters. As determined in this study, the $s^{\circ}_{20,w}$ of the unfolded subunit was 23.3 ± 0.3, the partial specific volume was 0.619 ± 0.006 ml/g, the intrinsic viscosity was 11.0 ± 0.2 ml/g, and the extinction coefficient at 260 nm was 145. The unfolded particles consisted of 33 ± 2% protein and 65 ± 2% RNA. Acrylamide gel electrophoresis indicated no loss of protein in the unfolded subunit.

The 30S subunit exhibits a decrease in sedimentation coefficient and an increase in intrinsic viscosity when exposed to low Mg^{++} concentration. The large change that occurs in these physical parameters indicates that the unfolded subunit is more asymmetric and/or hydrated than the 30S subunit. Based on the assumption that the hydration is unchanged from the 30S subunit, the 23S particle has a calculated axial ratio of approximately 7:1. The asymmetry of this particle can best be explained by assuming that a portion of the RNA chain swings out resulting in an extended conformation.

Solutions of the 23S particle were also subjected to sonication for 20-25 minutes in an attempt to break off the unfolded portion of the subunit. The sonication produced 3 particles that were isolated and analyzed for protein and RNA content. The three particles had approximate sedimentation coefficients of 5S, 10S, and 15S and were found to have protein/RNA ratios of 0.16, 0.49, and 0.49, respectively. From gel electrophoresis, it was found that the 10S particles had 13 proteins, and the 15S particles had 15 proteins. No protein bands were observed from the 5S particle. Unique proteins were found on the 10S and 15S particles. Four proteins in the 10S particle were not contained in the 15S particle, and six proteins in the 15S particle were not contained in the 10S particle. The sonication appears to break the unfolded subunit into at least two different particles, each of which contain a unique protein content.

REFERENCES

1. Allet, B., and P. F. Spahr, Eur. J. Biochem. 19, 250 (1971).

2. Atsmon, A., P. Spitnik-Elson, and D. Elson, J. Mol. Biol. 25, 161 (1967).

3. Barbieri, M., P. Pettazzoni, F. Bersani, and N. M. Maraldi, J. Mol. Biol. 54, 121 (1970).

4. Bickle, T. A., J. W. B. Hershey, and R. R. Traut, Proc. Nat. Acad. Sci. USA 69, 1327 (1972).

5. Bock, R. M., and W. C. Gillchriest, Fed. Proc. 17, 193 (1958).

6. Bodley, J. W., Biochemistry 8, 465 (1969).

7. Bohn, T. S., R. K. Farnsworth, and W. E. Dibble, Biochim. Biophys. Acta 138, 212 (1967).

8. Bolton, E. T., B. H. Hoyer, and D. B. Ritter, In Microsomal Particles and Protein Synthesis, p. 18, New York: Pergamon Press, 1958.

9. Brimacombe, R., J. Morgan, D. G. Oakley, and R. A. Cox, Nature New Biol. 231, 209 (1971).

10. Brimacombe, R., J. Morgan, and R. A. Cox, Eur. J. Biochem. 23, 52 (1971).

11. Brownlee, G. G., F. Sanger, and B. G. Barrell, Nature, 215, 735 (1967).

12. Bruskov, V. I., and N. A. Kiselev, J. Mol. Biol. 37, 367 (1968).

13. Bush, C. A., and H. A. Scheraga, Biochemistry 6, 3036 (1967).

14. Byers, B., J. Mol. Biol. 26, 155 (1967).

15. Cammack, K. A., and H. E. Wade, Biochem. J. 96, (1965).

16. Chang, F. N., and J. G. Flaks, Proc. Nat. Acad. Sci. USA 67, 1321 (1970).

17. Chao, F. C., and H. K. Schachman, Arch. Biochem. Biophys. 61, 220 (1956).

18. Chao, F. C., Arch. Biochem. Biophys. 70, 426 (1957).

19. Craven, G. R., and V. Gupta, Proc. Nat. Acad. Sci. USA 67, 1329 (1970).

20. Craven, G. R., P. Voynow, S. J. S. Hardy, and C. G. Kurland, Biochemistry 8, 2906 (1969).

21. Crichton, R. R., and H. G. Wittmann, Molec. Gen. Genet. 114, 95 (1971).

22. Davis, F. C., and B. H. Sells, J. Mol. Biol. 39, 503 (1969).

23. Dibble, W. E., and H. M. Dintzis, Biochim. Biophys. Acta 37, 152 (1960).

24. Doty, P., H. Boedtker, J. R. Fresco, R. Haselkorn, and M. Litt, Proc. Nat. Acad. Sci. USA 45, 482 (1959).

25. Duin, J. van, P. H. van Knippenberg, M. Dieben, and C. G. Kurland, Molec. Gen. Genet. 116, 181 (1972).

26. Dzionara, M., E. Kaltschmidt, and H. G. Wittmann, Proc. Nat. Acad. Sci. (Wash.) 67, 1909 (1970).

27. Ehresmann, C., and J. P. Ebel, Eur. J. Biochem. 13, 577 (1970).

28. Eikenberry, E. F., T. A. Bickle, R. R. Traut, and C. A. Price, Eur. J. Biochem. 12, 113 (1970).

29. Eilem, Y., and D. Elson, Biochemistry 10, 1489 (1971).

30. Fellner, P., Eur. J. Biochem. 11, 12 (1969).

31. Fellner, P., C. Ehresmann, and J. P. Ebel, Nature 225, 26 (1970).

32. Fellner, P., C. Ehresmann, and J. P. Ebel, Eur. J. Biochem. 13, 583 (1970).

33. Fogel, S., and P. S. Sypherd, Proc. Nat. Acad. Sci. USA 59, 1329 (1968).

34. Garrett, R. A., K. H. Rak, L. Daya, and G. Stoffler, Molec. Gen. Genet. 114, 112 (1971).

35. Gavrilova, L. P., D. A. Ivanov, and A. S. Spirin, J. Mol. Biol. 16, 473 (1966).

36. Gesteland, R. F., J. Mol. Biol. 18, 356 (1966).

37. Godson, G. N., and R. A. Cox, Biochim. Biophys. Acta 204, 489 (1970).

38. Gormly, J. R., C. Yang, and J. Horowitz, Biochim. Biophys. Acta 247, 80 (1971).

39. Guthrie, C., H. Nashimoto, and M. Nomura, Proc. Nat. Acad. Sci. USA 63, 384 (1969).

40. Hall, C. E., and H. S. Slayter, J. Mol. Biol. 1, 329 (1959).

41. Hardy, S. J. S., C. G. Kurland, P. Voynow, and G. Mora, Biochemistry 8, 2897 (1969).

42. Hart, R. G., Biochim. Biophys. Acta 60, 629 (1962).

43. Hart, R. G., Proc. Nat. Acad. Sci. USA 53, 1415 (1965).

44. Hill, W. E., J. W. Anderegg, and K. E. Van Holde, J. Mol. Biol. 53, 107 (1970).

45. Hill, W. E., G. P. Rossetti, and K. E. Van Holde, J. Mol. Biol. 44, 263 (1969).

46. Hill, W. E., J. D. Thompson, and J. W. Anderegg, J. Mol. Biol. 44, 80 (1969).

47. Hindennack, I., E. Kaltschmidt, and H. G. Wittmann, Eur. J. Biochem. 23, 12 (1971).

48. Hindennach, I., G. Stöffler, and H. G. Wittmann, Eur. J. Biochem. 23, 7 (1971).

49. Hosokawa, K., R. K. Fujimura, and M. Nomura, Proc. Nat. Acad. Sci. USA 55, 198 (1966).

50. Huang, K. H., and C. R. Cantor, J. Mol. Biol. 67, 265 (1972).

51. Huxley, H. E., and G. Zubay, J. Mol. Biol. 2, 10 (1960).

52. Itoh, T., E. Otaka, and S. Osawa, J. Mol. Biol. 33 109 (1968).

53. Jeffrey, P. D. and M. J. Pont, Biochemistry 8, 4597 (1969).

54. Kahan, L., and E. Kaltshcmidt, Biochemistry 11, 2691 (1972).

55. Kaltschmidt, E., Analyt. Biochem. 43, 25 (1971).

56. Kaltschmidt, E., M. Dzionara, D. Donner, and H. G. Wittmann, Molec. Gen. Genet. 100, 364 (1967).

57. Kaltschmidt, E., M. Dzionara, and H. G. Wittmann, Molec. Gen. Genet. 109, 292 (1970).

58. Kaltschmidt, E., and H. G. Wittmann, Proc. Nat. Acad. Sci. USA 67, 1276 (1970).

59. Kayushina, R. L., and L. A. Feigin, Bilfizika 14, 957 (1969).

60. Klug, A., K. C. Holmes, and J. T. Finch, J. Mol. Biol. 3, 87 (1971).

61. Kratky, O., H. Leopold, and H. Stabinger, Z. Angew, Phys. 27, 273 (1969).

62. Kurland, C. G., J. Mol. Biol. 2, 83 (1960).

63. Kurland, C. G., J. Mol. Biol. 18, 90 (1966).

64. Kurland, C. G., Science 169, 1171 (1970).

65. Kurland, C. G., Annual Review of Biochemistry, 337 (1972).

66. Kurland, C. G., M. Nomura, and J. D. Watson, J. Mol. Biol. 4 388 (1962).

67. Kurland, C. G., P. Voynow, S. J. S. Hardy, L. Randall, and L. Lutter, Cold Spr. Harb. Symp. Quant. Biol. 34, 17 (1969).

68. Lake, J. A., and H. S. Slayter, Nature 227, 1032 (1970).

69. Landridge, R., and K. C. Holmes, J. Mol. Biol. 5, 611 (1962).

70. Lengyel, P., and D. Söll, Bacteriol. Rev. 33, 264 (1969).

71. Lerman, M. I., A. S. Spirin, L. P. Gavrilovna, and V. F. Golov, J. Mol. Biol. 15, 268 (1966).

72. Littlefield, J. W., E. B. Keller, J. Gross, and P. C. Zamecnick, J. Biol. Chem. 217, 111 (1955).

73. Littlefield, J. W., and E. B. Keller, Fed. Proc. 15, 302 (1956).

74. Lowry, O. H., N. J. Rosebrough, A. J. Farr, and R. J. Randall, J. Biol. Chem. 193, 265 (1951).

75. Luria, S. E., M. Delbruk and T. F. Anderson, J. Bact. 46, 57 (1943).

76. Lutter, L. C., H. Zeichhardt, C. G. Kurland, and G. Stoffler, Molec. Gen. Genet. 119, 357 (1972).

77. Mangiarotte,, G., D. Apirion, D. Schlessinger, and L. Silengo, Biochemistry 7, 456 (1968).

78. Maruta, H., S. Natori, and D. Mizuno, J. Mol. Biol. 46, 513 (1969).

79. Matsura, S., Y. Tashiro, S. Osawa, and E. Otaka, J. Mol. Biol. 47, 383 (1970).

80. McPhie, P., and W. B. Gratzer, Biochemistry 5, 1310 (1966).

81. Mehl, J. W., J. L. Oncley, and R. Simha, Science 92, 132 (1940).

82. Mejbaum, W., Z. Physiol.Chem. 258, 117 (1939).

83. Meselson, M., M. Nomura, S. Brenner, C. Davern, and D. Schlessinger, J. Mol. Biol. 9, 696 (1964).

84. Miall, S. H., and F. O. Walker, Biochim. Biophys. Acta 174, 551 (1969).

85. Midgley, J. E. M., Biochim. Biophys. Acta 108, 340 (1965).

86. Mizushima, S. and M. Nomura, Nature 226, 1214 (1970).

87. Möller, W., and A. Chrambach, J. Mol. Biol. 23,377 (1967).

88. Moore, P. B., J. Mol. Biol. 60, 169 (1971).

89. Moore, P. B., R. R. Traut, M. Noller, P. Pearson, and H. Delius, J. Mol. Biol. 31, 441 (1968).

90. Mora, G., D. Donner, P. Thammana, L. Lutter, and C. G. Kurland, Molec. Gen. Genet. 112, 229 (1971).

91. Morgan, J., and R. Brimacombe, Eur. J. Biochem. 29, 542 (1972).

92. Mottet, N. K., and S. P. Hammar, J. Cell Sci. 11, 403 (1972).

93. Nashimoto, H., W. Held, E. Kaltschmidt, M. Nomura, J. Mol. Biol. 62, 121 (1971).

94. Natori, S., H. Maruta, and D. Mizuno, J. Mol. Biol. 38, 109 (1968).

95. Nomura, M., Bacteriol. Rev. 34, 228 (1970).

96. Nomura, M., M. Ozaki, P. Traub, and C. V. Lowry, Cold Spr. Harb. Symp. Quant. Biol. 34, 49 (1969).

97. Nomura, M., P. Traub, and H. Bechmann, Nature 219, 793 (1968).

98. Ortega, J. P., and W. E. Hill, Biochemistry 12, 3241 (1973).

99, Osawa, S., Ann. Rev. Biochem. 37, 109 (1968).

100. Osawa, S., E. Otaka, T. Itoh, and T. Fukui, J. Mol. Biol. 40, 321 (1969).

101. Palade, G., J. Biophys. Biochem. Cytol. 1, 59 (1955).

102. Palade, G., and P. Siekewitz, J. Biophys. Biochem. Cytol. 2, 171 (1956).

103. Palade, G., and P. Siekewitz, J. Biophys. Biochem. Cytol. 2, 671 (1956).

104. Perrin, F., J. Phys. Radium 7, 1 (1936).

105. Petermann, M. L. and M. G. Hamilton, Cancer Research 12, 373 (1952).

106. Petermann, M. L. and M. G. Hamilton, J. Biol. Chem. 224, 723 (1957).

107. Roark, D. E., and D. A. Yphantis, Biophys. J. 8, A99 (1968).

108. Rodgers, R., Biochem. J. 90, 548 (1964).

109. Roth, H. E., and K. H. Nierhaus, FEBS Letters, 31 35 (1973).

110. Santer, M., and M. Szekly, Biochemistry 10, 1841 (1971).

111. Sarkar, P. K., J. T. Yang, and P. Doty, Biochemistry 5, 1 (1967).

112. Scafati, A. R., M. R. Stornaiuolo, and P. Novaro, Biophys. J. 11, 370 (1971).

113. Schachman, H. K., A. B. Pardee, and R. Y. Stanier, Arch. Biochem. Biophys. 38, 245 (1954).

114. Schendel, P., P. Maeba, and G. R. Craven, Proc. Nat. Acad. Sci. USA, 69, 544 (1972).

115. Schlessinger, D., J. Mol. Biol. 2, 92 (1960).

116. Schaup, H. W., M. Green, and C. G. Kurland, Molec. Gen. Genet. 109, 193 (1970).

117. Schaup, H. W., and C. G. Kurland, Molec. Gen. Genet. 114, 350 (1972).

118. Schaup, H. W., M. Sogin, C. Woese, and C. G. Kurland, Molec. Gen. Genet. 114, 1 (1971).

119. Serdyuk, I. N., N. I. Smirnov, O. B. Ptitsyn, and B. A. Fedorov, FEBS Letters 9, 324 (1970).

120. Smith, W. S., Ph.D. Thesis, University of Wisconsin 1971.

121. Spirin, A.S., and L. P. Gavrilovna, Mol. Biol. Biochem. Biophys. 4 (1969).

122. Spirin, A. S., N. A. Kisselev, R. S. Shakulov, and A. A. Bogdanov, Biokhimia 28, 920 (1963).

123. Spitnik-Elson, P., and A. Atsmon, J. Mol. Biol. 45, 113 (1969).

124. Staehelin, T. and Maglott, D. R., in: Methods in Enzymology Vol. XX, Part C, Eds. K. Moldove and L. Grossman.

125. Staehelin, T., and M. Meselson, J. Mol. Biol. 16, 245 (1966).

126. Stanley, W. M., Jr., Ph.D. Thesis, University of Wisconsin (1963).

127. Stanley, W. M., Jr., and R. M. Bock, Biochemistry 4, 1302 (1965).

128. Stanley, W. M., Jr., M. Salas, A. J. Wahba, and S. Ochoa, Proc. Nat. Acad. Sci. USA 56, 290 (1966).

129. Stöffler, G., L. Daya, K. H. Rak, and R. A. Garrett, J. Mol. Biol. 62, 411 (1971).

130. Stöffler, G., and H. G. Wittmann, Proc. Nat. Acad. Sci. USA 68, 2283 (1971).

131. Stöffler, G., R. Hasenbank, M. Lütgehaus, R. Maschler, C. A. Morrison, H. Zeichhardt, and R. A. Garrett, Molec. Gen. Genet. 127, 89 (1973).

132. Svedberg, T., and K. O. Pedersen, The Ultracentrifuge (Clarendon Press, Oxford, 1940).

133. Tal, M., Biochim. Biophys. Acta 169, 564 (1968).

134. Tal, M., Biochemistry 8, 424 (1969).

135. Tal, M., Biochim. Biophys. Acta 224, 470 (1970).

136. Teller, D. C., T. A. Horbett, E. G. Richards, and H. K. Schachman, Ann. N. Y. Acad. Sci. 164, 66 (1969).

137. Tissières, A., J. D. Watson, D. Schlessinger, and B. R. Hollingworth, J. Mol. Biol. 1, 221 (1959).

138. Traub, P., and M. Nomura, J. Mol. Biol. 34, 575 (1968).

139. Traub, P., and M. Nomura, Proc. Nat. Acad. Sci. USA 59, 777 (1968).

140. Traub, P., and M. Nomura, J. Mol. Biol. 40, 391 (1969).

141. Traut, R. R., H. Delius, C. Ahmad - Zadek, T. A. Bickle, P. Pearson, and A. Tissières, Cold Spr. Harb. Symp. Quant. Biol. 34, 25 (1969).

142. Traut, R. R., P. B. Moore, H. Delius, H. Noller, and A. Tissières, Proc. Nat. Acad. Sci. USA 57, 1294 (1967).

143. Tso, P. O. P., J. Bonner, and J. Vinograd, J. Biophys. Biochem. Cytol. 2, 451 (1956).

144. Tso, P. O. P., J. Bonner, and J. Vinograd, Biochem. Biophys. Acta 30, 570 (1958).

145. Vasiliev, V. D., FEBS Letters 14, 203 (1971).

146. Voynow, P., and C. G. Kurland, Biochemistry 10, 517 (1971).

147. Waller, J. P., and J. I. Harris, Proc. Nat. Acad. Sci. USA 47, 18 (1961).

148. Weber, H. J., Mol. Gen. Genet. 119, 233 (1972).

149. Weller, D. L., and J. Horowitz, Biochim. Biophys Acta 87, 361 (1964).

150. Weller, D. L., Y. Schechter, D. Musgrave, M. Rougvie, and J. Horowitz, Biochemistry 7, 3668 (1968).

151. Wittmann, H. G., G. Stoffler, I. Hindennach, C. G. Kurland, L. Randall-Hazelbauer, E. A. Birge, M. Nomura, E. Kaltschmidt, S. Mizushima, R. R. Traut and T. A. Bickle, Mol. Gen. Genet. 111, 327 (1971).

152. Yphantis, D. A., Biochemistry 3, 297 (1964).

153. Zimmermann, R. A., A. Muto, P. Fellner, C. Ehresmann, and C. Branlant, Proc. Nat. Acad. Sci. USA 69 1282 (1972).

154. Zubay, G., and M. H. F. Wilkins, J. Mol. Biol. 2 105 (1960).